The LINNEAN SOCIETY of London ZOOLOGICAL Journal of the Linnean Society

Zoological Journal of the Linnean Society, 2016. With 7 figures

Geographical variation in head shape of a Neotropical group of toads: the role of physical environment and relatedness

LUCAS N. BANDEIRA[1]*, JOÃO ALEXANDRINO[2], CÉLIO F. B. HADDAD[1] and MARIA TEREZA C. THOMÉ[1]

[1]*Departamento de Zoologia, Instituto de Biociências, Universidade Estadual Paulista 'Julio de Mesquita Filho', Rio Claro São Paulo, 13506-900, Brazil*
[2]*Departamento de Ciências Biológicas, Universidade Federal de São Paulo, Diadema São Paulo, 09972-270, Brazil*

Received 28 May 2015; revised 26 April 2016; accepted for publication 29 April 2016

In this study we review the morphological variation within the *Rhinella crucifer* species group using geometric morphometrics. We sampled 270 specimens from 78 localities comprising all genetic units delimited for the group. We placed 12 landmarks and 89 semi-landmarks defining morphological structures of the anterior region of the body (head and parotoid glands) on standardized photographs of dorsal aspects of specimens. We checked for the existence of size-free morphological variation using exploratory multivariate analyses and tested for differences among categories (genetic units) using canonical variate analyses. We investigated the effects of relatedness by conducting canonical analyses hierarchically, and tested for phylogenetic signal using reconstruction of morphologies on a tree derived from mitochondrial data. We then corrected for relatedness using phylogenetic principal component analysis, and tested for the influence of the physical environment (temperature, humidity and altitude) with a partial Mantel test of matrix correlation. Our results revealed that there is size-free shape variation in the group. Shape changes are related to specific structures in the head, with landmarks and semi-landmarks highlighting changes in a complementary way. We were able to statistically detect the effect of phylogenetic distance with landmarks when considering the closest genetic units as a single category. A significant proportion of the variation in head shape can be explained by environmental variables, suggesting that conditions of the physical environment should also be considered as a source of morphological variation.

doi: 10.1111/zoj.12460

ADDITIONAL KEYWORDS: Brazilian Atlantic forest – geometric morphometrics – phylogenetic principal component analysis – phylogenetic signal – *Rhinella crucifer* group – semi-landmarks.

INTRODUCTION

The Brazilian Atlantic forest possesses remarkable biodiversity, and the origins of its biota have been the subject of many evolutionary studies in the last decade (Turchetto-Zolet *et al.*, 2013). The number of amphibian species occurring in this biome is outstanding, with over 500 recorded (Haddad *et al.*, 2013). The *Rhinella crucifer* group of toads is one of the most emblematic components of this anurofauna, as its species are abundant across the Atlantic forest domain (Baldissera, Caramaschi & Haddad, 2004). The first species belonging to this group was described by Wied-Neuwied (1821) as *Bufo crucifer*, but morphological variations among populations attributed to this taxon have been confusing taxonomists over the years, resulting in a list of names and synonyms (Baldissera *et al.*, 2004; Frost, 2014). Many of these forms were described based upon characters with limited or no phylogenetic signal, such as the cross-shaped colour pattern often present on the dorsum and for which the group is named (Baldissera *et al.*, 2004).

*Corresponding author. E-mail: azebandeira@gmail.com

Baldissera *et al.* (2004) revised the taxonomy of the *Rhinella crucifer* group on the basis of external morphology and traditional morphometric analyses. In that study the authors made use of a broad sampling effort to delimit five species under the morphological species concept. Three of these species were retained by Baldissera *et al.* (2004), namely *Rhinella crucifer* (Wied-Neuwied, 1821), *Rhinella ornata* (Spix, 1824) and *Rhinella henseli* (Lutz, 1934). The two remaining species were described as *Rhinella abei* and *Rhinella pombali* (Baldissera *et al.*, 2004). For each of these species the authors inferred a non-overlapping geographical distribution (Baldissera *et al.*, 2004), subsequently further extended by other authors (Lima *et al.*, 2005; Silveira, Salles & Pontes, 2009). Later, Vaz-Silva, Valdujo & Pombal (2012) described a sixth species for the group, *Rhinella inopina*, restricted to Atlantic forest enclaves in the Cerrado biome domain.

In a recent survey, Thomé *et al.* (2012) combined multilocus sequence data with intensive sampling across the group's distribution to examine the genetic structure in the *Rhinella crucifer* group. Thomé *et al.* (2012) employed trees and frequency-based approaches to find five genetic units whose geographical distributions challenged the prevailing taxonomy. Correspondence between genetically distinguishable units and recognized species was straightforward only for *R. henseli* and *R. inopina*, while for *R. crucifer* and *R. ornata* the species ranges and the distributions of genetic groups overlapped only partially. *Rhinella abei* appeared nested within *R. ornata*, and *R. pombali* was synonymized to *R. ornata* and *R. crucifer*, as its distribution is largely concordant with a hybrid zone between the latter two species. Additionally, Thomé *et al.* (2012) suggested the existence of a divergent population pending taxonomic evaluation, recently elevated to species status under the name *Rhinella casconi* by Roberto, Brito & Thomé (2014).

One possible explanation for the disparity between genetically and morphologically defined groups in the *Rhinella crucifer* group is the variation in body size (snout–vent length – SVL) over its geographical distribution. Morphometric multivariate analyses in Baldissera *et al.* (2004) show that most of the variation in the group is associated with this variable, raising the possibility that size acted as a confounding factor in the morphometric analyses that may otherwise support taxonomic decisions for the group. Furthermore, morphometric studies on anurans have reported variation that covaries with variation in environmental conditions (Castellano & Giacoma, 1998; Castellano *et al.*, 1999; Rosso, Castellano & Giacoma, 2004; Schauble, 2004; Kutrup, Bulbul & Yilmaz, 2006; Marcelino, Haddad & Alexandrino, 2009), raising the possibility that local climates might also play a role in generating phenotypic differentiation within the *R. crucifer* group.

In contrast to traditional morphometrics, geometric morphometrics allows for the quantification of pure shape through the definition of homologous landmarks, contours of structures and the use of a statistical formalism that expresses shape change directly as deformation (Bookstein, 1991). Therefore, size-free variation in complex morphological structures is effectively quantified in terms of localized and hierarchical shape phenomena captured at different geometric scales (Bookstein, 1996; Rohlf, Loy & Corti, 1996; Dryden & Mardia, 1998). In this study we used geometric morphometrics to reassess morphometric variation in the *Rhinella crucifer* group and to consider its evolutionary history and local variation relative to environmental conditions (climate and altitude). Our main questions are: (1) Is there size-free shape variation in the group? (2) If so, can this variation be explained by genetic relatedness? (3) Is shape variation influenced by local variation of the physical environment?

MATERIAL AND METHODS

Sampling

We gathered 270 specimens of the *R. crucifer* group from 78 localities (Fig. 1, Appendix 1). Specimens are deposited in the following institutions: 'Célio Fernando Baptista Haddad' amphibian collection, CFBH (Departamento de Zoologia, Instituto de Biociências – IB, Universidade Estadual Paulista – UNESP, Rio Claro, SP, Brazil); herpetological collection of the 'Instituto de Investigación Biológica del Paraguay', IIBPH (Asunción, Paraguay); Museum of Zoology University of São Paulo, MZUSP (Universidade de São Paulo – USP, São Paulo, SP, Brazil); and the Museum of Natural Sciences of the Pontifícia Universidade Católica, MCNPUC-MG (Pontifícia Universidade Católica de Minas Gerais – PUCMG, Belo Horizonte, MG, Brazil). The distributions of body sizes of the different subsets of the sample are illustrated in Figure 2.

According to the results of Thomé *et al.* (2012), in several cases current taxonomy does not represent evolutionary units in the *Rhinella crucifer* group and so we assigned each specimen to their respective genetic unit (G, N, P, C, c1 and S; Thomé *et al.*, 2012). Assignment was determined genetically, as many of the specimens were used in a previous phylogenetic analysis or originated from the same populations, or, in a few cases, by their geographical origin. Individuals from the transition zone between

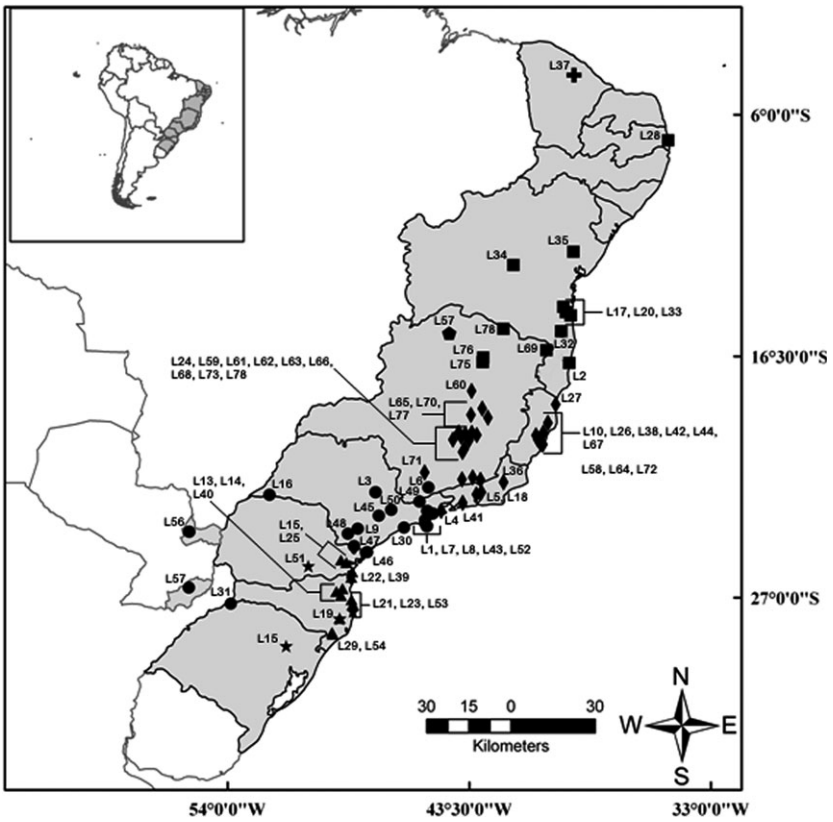

Figure 1. Localities in Brazil and Paraguay sampled in this study. (see Appendix for latitude, longitude and administrative district). Cross, unit G; square, unit N; pentagon, unit P; diamond, unit H; circle, unit C, triangle, unit c1; star, unit S.

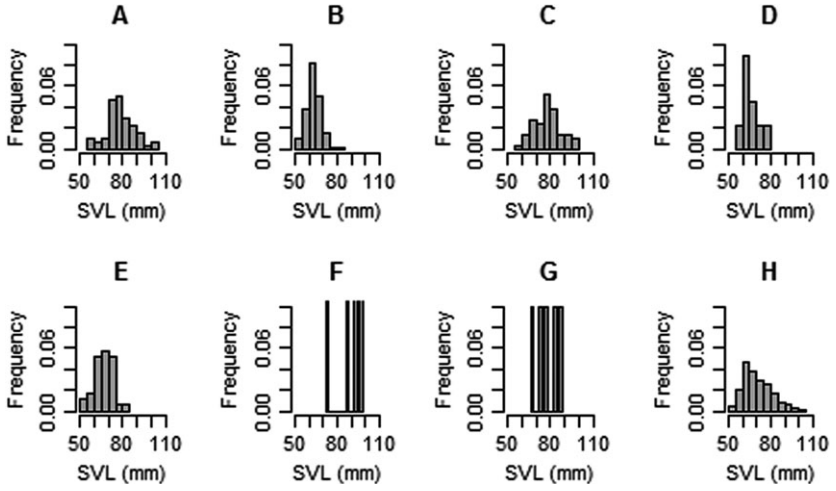

Figure 2. Histograms illustrating body size distribution of the different subsets of the sample. A, unit 'N'; B, unit 'C'; C, unit 'H'; D, unit 'S'; E, unit 'c1'; F, unit 'P'; G, unit 'G'; H, all species together.

N and C (putative hybrids) were included in a separate category (H). Because species in the group show sexual dimorphism in size, we restricted all analyses to males with well-developed secondary sexual characteristics (presence of nuptial pads and hypertrophied arms relative to females of similar sizes).

Data acquisition

We obtained photographic images for all individuals, adapting the methodology described by Ivanović *et al.* (2008). We positioned each specimen with its jaw line parallel to the photographic plane and obtained head images with a Canon Power Shot G9 digital camera fixed over the photographic plane 20 cm from the specimen at 12-megapixel resolution and with macro function. We positioned each specimen at the centre of the optical field to reduce and equalize distortion. We chose to investigate head shape because it includes many characters used in studies of intra- and interspecific variation of amphibians (e.g. Clemente-Carvalho *et al.*, 2008, 2011; Vieira *et al.*, 2008; Ivanović *et al.*, 2009, 2011).

With the obtained images we created two separate data sets, one consisting of 12 landmarks positioned on each specimen: (1) top of the rostrum, (2) beginning of the loreal crest, (3) junction point between the loreal crest and the anterior edge of the eye, (4) junction point between the supra-tympanic edge and posterior edge of the eye, (5) midpoint between landmarks '3' and '4', (6) top of the paratoid gland, (7) bottom of the paratoid gland, (8) beginning of the supra-tympanic edge, (9) beginning of the cephalic crest, (10) end of the cephalic crest, (11) midpoint of the loreal crest and (12) landmark positioned in the mandible at 90° degrees point '11' (Fig. 3A); and another with 89 semi-landmarks (Fig. 3B). While landmarks are used on homologous, unambiguous, repeatedly identifiable structures, semi-landmarks are points with estimated positions (Bookstein, 1997; Adams, Rohlf & Slice, 2004; Mitteroecker & Gunz, 2009; Clemente-Carvalho *et al.*, 2011), generally used when landmarks alone cannot describe biological forms or patterns (Oxnard, 1978). We used semi-landmarks to characterize the following regions: the mandibular arch (MA), supra-tympanic edge (STe), inner edge of the eye (ieE), loreal crest (LC) and parotoid gland (PG) (see Fig. 3B). Because spacing between semi-landmarks is arbitrary (Croix *et al.*, 2011), we aligned these configurations with a perpendicular projection (Sampson *et al.*, 1996; Bookstein *et al.*, 2002; Sheets, Keonho & Mitchell, 2004). In this method, the differences in semi-landmark positions between the reference and each specimen configuration are removed by estimating the

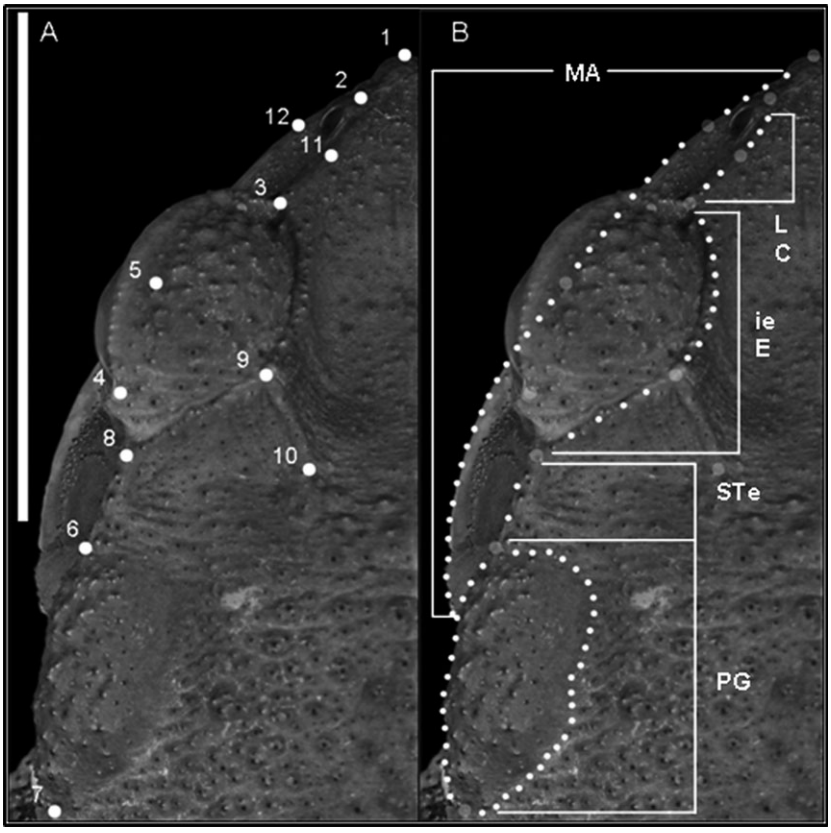

Figure 3. Landmarks (A) and semi-landmarks (B) used in this study (see text for details) plotted on the head of specimens of the *Rhinella crucifer* group (CFBH 18815, Teresópolis, RJ). Scale bar = 25 mm.

distinction tangential to the curve and removing the component of the difference that lies along this tangent (Sheets *et al.*, 2004). We used the TPS relative warps (TpsRW) software version 1.44 (Rohlf, 2005) to slide the semi-landmarks along their respective curves and minimize the distances between subject and reference (Bookstein *et al.*, 2002; Clemente-Carvalho *et al.*, 2011).

The choice of landmarks and semi-landmarks used here was based on diagnostic characters defined for the different species in the group as a whole (Baldissera *et al.*, 2004; Vieira *et al.*, 2008; Vaz-Silva *et al.*, 2012). We positioned the landmarks and semi-landmarks on images of each specimen (the same image being used for each procedure), with the program TPSdig2 (http://life.bio.sunysb.edu/morph) (Rohlf, 2004, 2005). Aiming to control possible sources of error, all landmarks and semi-landmarks were positioned by the same person (L.N.B.).

Data analyses

Erroneous placement of landmarks can lead to spurious interpretation of the patterns and processes under investigation. In this scenario, quantification of measurement error is an important step for morphometric work. We quantified error by employing the Procrustes ANOVA (Goodall, 1991; Klingenberg & Monteiro, 2005). For this, we positioned landmarks twice in a subsample consisting of 70 randomly selected specimens. We then subjected both datasets to a Generalized Procrustes Analysis (GPA, commonly known as 'Procrustes fit', see below), and the Procrustes-fitted configurations were used in repeated-measures Procrustes ANOVA. The measurement error is the percentage of variation resulting from the division between the mean square error (MSE) by the mean square (MS) of the lowest level of biological significance (in the specific case: individuals) (see Table 1). We assumed that error below 30% is acceptable. All analyses were performed in the software MorphoJ Version 2.0 (Klingenberg, 2011).

To describe and quantify variation in shape within the group we first statistically control for the effects of body size on the landmark and semi-landmark data. For this step we applied standard geometric morphometric approaches to align the configurations of landmarks and semi-landmarks before any analysis. We conducted a GPA to align the landmark configurations of all specimens with the software MorphoJ Version 2.0 (Klingenberg, 2011). The GPA preserves all information about shape variability among specimens while removing information unrelated to shape (position, scale and orientation) (Clemente-Carvalho *et al.*, 2008, 2011; Ivanović *et al.*, 2008). After a multivariate regression of the landmark and semi-landmark data, a ln(centroid size) was performed with the same software. MorphoJ allows pooling of variance by taxonomic unit or geographical unit in the computation of the regression statistics, and a permutation test is available for assessment of the probability of the regression (if it is rejected, no further size adjustment is necessary). As the results of the regressions performed were not significant (see Data S1), no allometric correction was necessary and the coordinates resulting from the Procrustes superimposition were used in further analyses. A plot of head length against body length was included as a complement to the multivariate regression (see Fig. 4).

To determine if there is variation in shape among the group as a whole and to explore the relative amount of variation in cranial shape, we used a variance–covariance matrix and performed a principal components analysis (PCA) (Bookstein, 1991; Rohlf, 1993; Clemente-Carvalho *et al.*, 2011). Principal components were used as new shape variables to reduce the dimensionality of the dataset and to produce independent variables (Baylac & Friess, 2005). We visualized the principal cranial shape differences among the species on deformation grids (Rohlf, 1993; Adams *et al.*, 2004; Klingenberg, 2013) created in the software MorphoJ Version 2.0 (Klingenberg, 2011). In addition, to ascertain whether changes in form are sufficient to differentiate between

Table 1. Procrustes ANOVA results

Effect	SS	MS	d.f.	*F*	*P*	%Variance
Individual	0.33457990	0.0009293886	18	6.09	<0.0001	
Replicates	0.03445240	0.0017226619	1	0.99	0.3323	1.8535
Residual	0.96664140	0.0002543793	190			

Mean square (MS) is the amount of variation from the one higher level in the hierarchy. The *F* values represent the comparison of each MS to the one lower level of MS which could be the source of error. %Variance represents the division of the mean square of the lowest level of biological significance by the mean square error for the ANOVA.

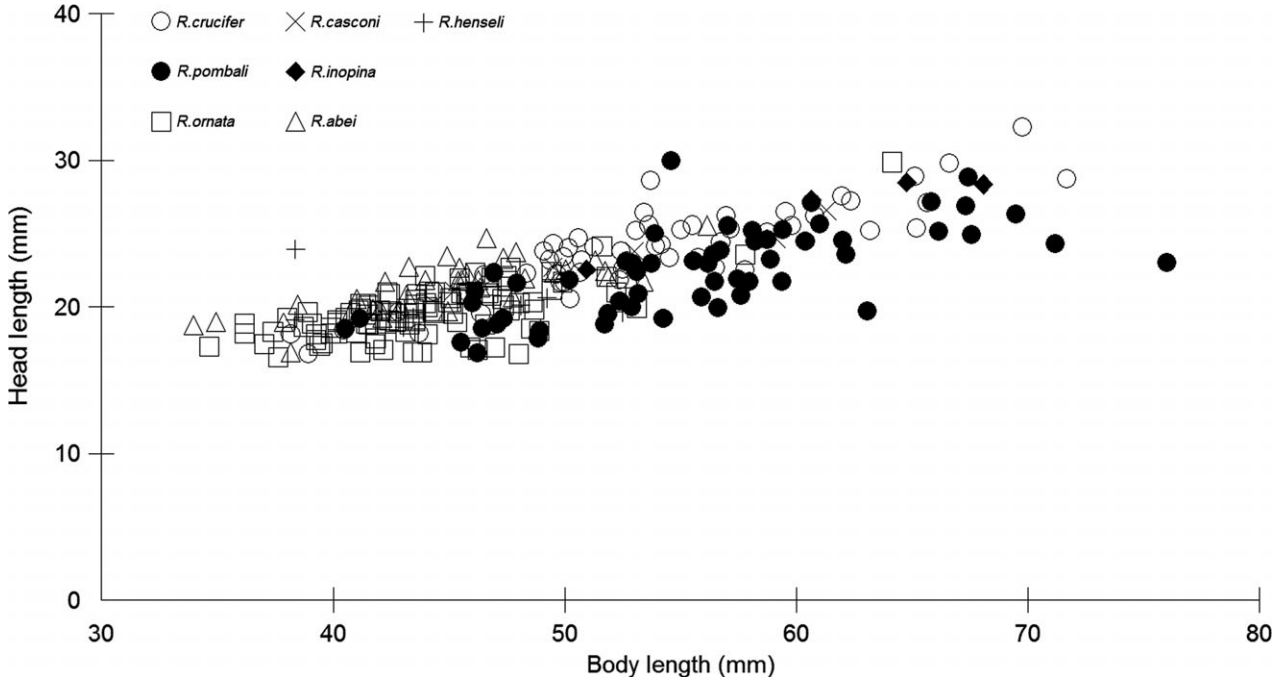

Figure 4. Scatterplot of head length against body length. Body length = snout–vent length – head length.

predefined categories, we used canonical variate analyses (CVAs), with paired permutation tests based on Procrustes and Mahalanobis distances (Gould & Johnston, 1972). To first explore the effects of relatedness we performed CVA considering all genetic categories separately (G, P, N, C, S, H and c1), and then proceeded with CVA hierarchically by clustering categories according to genetic relatedness (following the topology in Thomé *et al.*, 2012; Fig. 5). Finally, we performed a CVA including only the closest genetic units according to mitochondrial DNA genetic distances in Thomé *et al.* (2012). We conducted permutation tests with 10 000 permutations. For all CVA and permutation tests we used the software MorphoJ Version 2.0 (Klingenberg, 2011).

To further investigate how phylogenetic history affects variation in head shape, we first mapped the principal components on a phylogeny using Maddison's method (Maddison, 1991; McArdle & Rodrigo, 1994; Rohlf, 2001). Two phylogenetic trees for the *Rhinella crucifer* group were used, one with topology based on the original mitochondrial DNA (putative hybrids not included, Fig. 5A), and an alternative tree with the closest genetic units included as a collapsed clade (putative hybrids included, Fig. 5B). The phylogenetic trees have been superimposed onto a plot of the first two principal components (PC1 and PC2) derived from the variance–covariance matrix among all specimens used as representatives of clades. To test for phylogenetic signal we reconstructed the morphometric data for ancestral nodes of the trees with squared-change parsimony (Maddison, 1991; Cole, Lele & Richtsmeier, 2002; MacLeod, 2002; Cardini & Elton, 2008; Klingenberg & Gidaszewski, 2010). The null hypothesis (absence of phylogenetic signal) was then simulated by permutation: specimen configurations are randomly reassigned to the terminal nodes of the phylogeny and then mapped onto the phylogeny to calculate the total tree length in units of morphometric distance. The proportion of permuted data sets in which the sum of squared changes is shorter or equal to the value obtained for the original data is the *P* value for the test. For reconstruction of the morphometric data and tests of phylogenetic signal we used the MorphoJ software Version 2.0 (Klingenberg, 2011).

Second, we explored shape variation controlling for phylogenetic covariance with a phylogenetic PCA (pPCA) (Revell, 2009; Polly *et al.*, 2013). We used pPCA both to explore the shape variation that is free from phylogenetic signal and to relate it to environmental factors. The pPCA is similar to ordinary PCA, but the covariance matrix is inversely weighted by the phylogeny and the space is centred on the estimated phenotype of the root node of the tree. The inverse weighting of the pPCA corrects for shared phylogenetic history in constructing the axes, producing scores that represent the remaining variation. We then contrasted the values of the first two phylogenetic principal components of each specimen

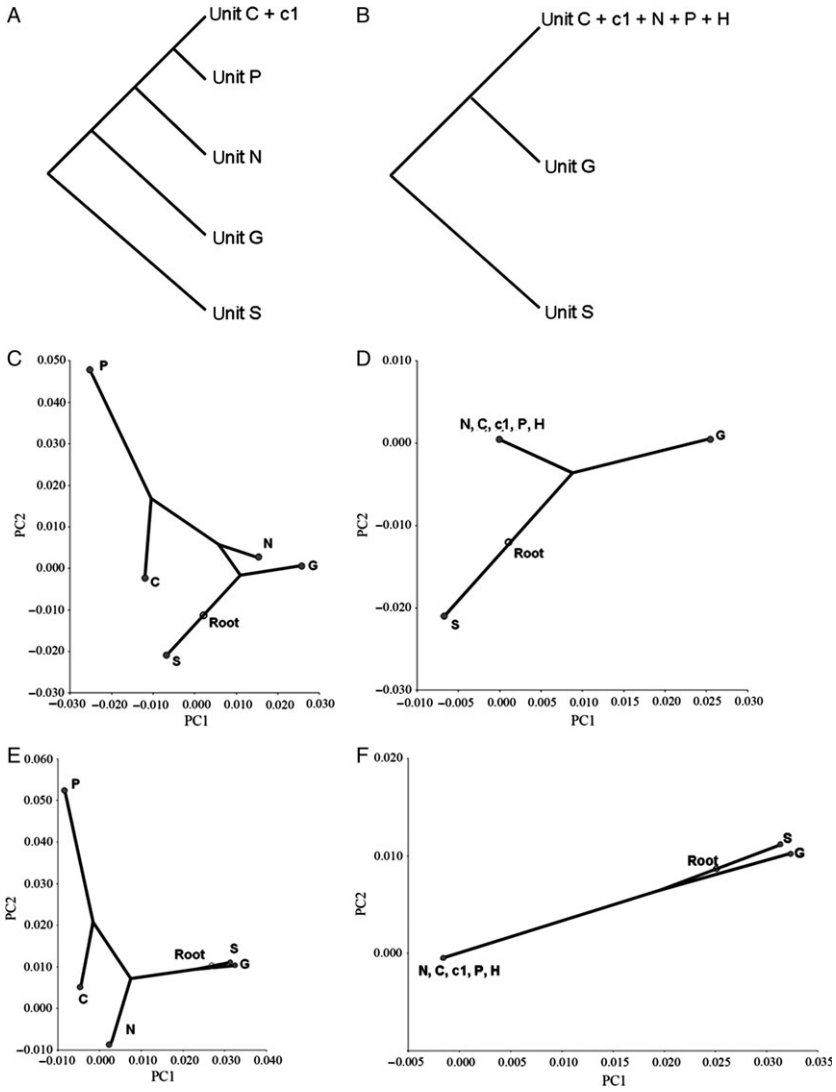

Figure 5. Phylogenetic trees for the *Rhinella crucifer* group considered in this study. A, topology of the original mitochondrial DNA tree from Thomé *et al.* (2012); B, alternative tree with closest genetic units collapsed into a single clade. C–F, plots showing reconstruction of evolutionary changes in head shape of the species of the *Rhinella crucifer* group according to both mitochondrial trees. C, reconstruction using landmarks and the original tree; D, reconstruction using landmarks and collapsed tree; E, reconstruction using semi-landmarks and the original tree; F, reconstruction using semi-landmarks and collapsed tree.

against environmental distance using partial Mantel tests (Smouse, Long & Sokal, 1986) (see below). For the pPCA analyses, and to generate the graphs, we used the RStudio language and environment for statistical computing version 5.13 for Windows (R Development Core Team, 2014; http://www.R-project.org) and the packages ape (Paradis, Claude & Strimmer, 2004) and phytools (Revell, 2009, 2012), for the R environment.

Finally, to test the influence of physical environment on morphology, we applied the partial Mantel test of matrix association (Smouse *et al.*, 1986). We used the matrix of scores generated by pPCA as the dependent matrix. The independent matrix was that of the environmental data. Between-locality environmental distance was expressed by pairwise simple Euclidean distance for a set of environmental variables that are not significantly correlated and that describe elevation and climate (Gvozdík, Moravec & Kratochvíl, 2008) in the Brazilian Atlantic forest (Marcelino *et al.*, 2009). The environmental variables were elevation (Alt), annual mean temperature (AnnMTemp), temperature annual range (TemAnnRge), annual precipitation (AnnPrec), precipitation of the

wettest month (PreciWetMon) and precipitation of the wettest quarter (PrecWetQtr), and were obtained from the bioclimatic database 'Worldclim' at a spatial resolution of 30 arc-seconds (http://www.worldclim.org/) (Hijmans *et al.*, 2005). The macroclimatic data of 'TemAnnRge' and 'AnnPrec' show the annual climate cycle experienced by a population (Gvozdík *et al.*, 2008). The partial Mantel tests were performed with 10 000 randomizations and $\alpha = 5\%$ in the package Ecodist 1.2.9 (Goslee & Urban, 2007) in the RStudio language and environment for statistical computing version 5.13 for Windows (R Development Core Team, 2014, http://www.R-project.org). For both analyses we considered the original mitochondrial DNA (putative hybrids not included, Fig. 5A) and an alternative tree with the closest genetic units included as a collapsed clade (putative hybrids included, Fig. 5B).

RESULTS

Procrustes ANOVA was performed for total of 70 specimens of and the proportion of variation related to this effect was low (see Table 1). Each specimen was imaged once and each image was digitized twice, producing 140 raw coordinate data for the head. Measurement error was estimated from this Procrustes ANOVA by considering individual as the main source of variation, nested by variation in digitized replicates, and residuals.

In the PCA with landmark data the two-first components explained 52.5% of the variation in head shape. The biplot shows overlap of the clouds of points representing all genetic units, as shown in the Supporting Information (Data S2A). Changes in shape, depicted by the first principal components, mainly encompass displacement of landmarks representing the cephalic crests and eye, as shown in the deformation grids (Fig. 6). Specimens from genetic categories N and H display more prominent and well-developed cephalic crests while the specimens from C, c1 and S display gradually underdeveloped crests, respectively. The representatives of category G have less conspicuous cephalic crests. Individuals of categories N, C and H also present similar, broader eyes, while G, P and S display smaller and narrower eyes. For the semi-landmarks, the two-first components explained 38.3% of the total variance and the categories in the biplot are also broadly overlapping, as shown in Data S2B. The main changes in shape consist of the displacement of the parotoid gland and the eye, with some differences related to the contours of the mandibular arch. Specimens of categories N, C and H have similar spherical parotoid glands of larger size whereas S specimens display a thinner and longer parotoid gland. G and P also display discrepant paratoid shapes, smaller than in the other groups and much broader anteriorly in G, and with two distinguishable lobes in P (Fig. 6).

In the CVA performed with landmarks, the first two canonical variates accommodated 70.73% of the variation when all genetic units were considered separately, with the confinement of the scores for category S to more peripheral regions of the multivariate space (Fig. 7A). In the CVA with only phylogenetically closest units (categories N, P, H, C and c1), the first and second variates accommodated 75.09% of the variation and showed slightly better separation of categories P and G, although with overlap (Fig. 7B). Finally, in the CVA including clustered genetic units (categories [N, P, H, C, and, c1]) plus G and S, the first two canonical variables accommodated 91.79% of the variation and there was little overlap among all categories in the biplot (Fig. 7C). In the CVAs performed with the semi-landmark dataset, the first two canonical variables accommodated 52.62, 60.16 and 82.17% of the total variation in the analyses considering all units separately, considering only the closest genetic units and considering clustered genetic units together, respectively. In the first, the biplot shows some overlap of categories N, P, H, C and c1, and clear isolation of categories S and G (Fig. 7D). In the second CVA there is almost complete separation of N and H, and overlap of the remaining categories (Fig. 7E), whereas the third biplot shows complete isolation of categories (Fig. 7F). Permutation tests based on Mahalanobis distances support that the variation in form is sufficient to differentiate among the considered categories, whereas permutation tests performed using Procrustes distances did not yield significant results in some comparisons involving categories G, c1 and P (Table 2).

Mapping of the scores of the first two principal components of the landmark dataset onto the two alternative phylogenies yielded different results. In the reconstruction of shape based on the original phylogeny, the plot shows a conspicuous divergence between the genetic category P and the others, described by the second principal component (Fig. 5C), whereas differences between C and S and between N and G are described by the first principal component. The null hypothesis of no phylogenetic signal could not be rejected ($P = 0.282$, Table 3). The reconstruction onto the collapsed phylogeny shows a clear divergence between categories [N, P, H, C and c1], G and S. [N, P, H, C and c1] and G, and S and G, are distinguished primarily by the first principal component (Fig. 5D). Between categories [N, P, H, C and c1] and S the divergence lies mainly in the second component. The permutation test confirmed significant phylogenetic structure in the data ($P < 0.0001$,

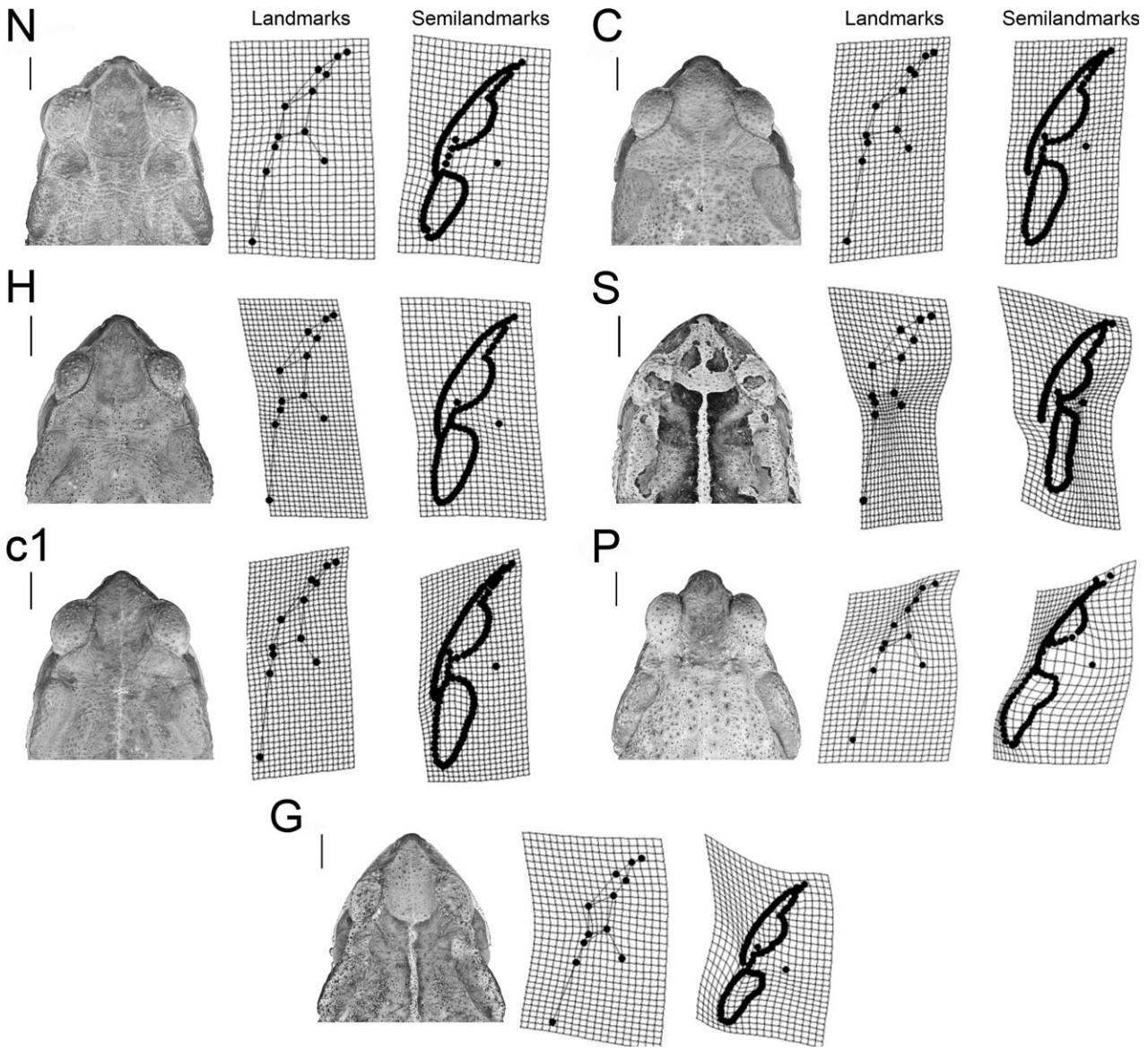

Figure 6. Images of the dorsum of the head of representatives of each analysed category of the *Rhinella crucifer* group and corresponding deformation grids implied by the first principal component. N, North unit (CFBH = 2583); C, Center unit (CFBH = 15383); H, 'Hybrids' (PUC = 7537); S, South unit (CFBH = 20277); c1, centre 1 unit (subclade) (CFBH = 18175); P, 'Peruacu' unit (MZUSP = 142105); G, 'Guaramiranga' unit (CFBH = 28172).

Table 3). In the analysis generated with semi-landmarks and the original phylogeny, the plot shows a similar disposition as for the analysis with landmarks (Fig. 5E). Overall there is a clear distinction between [N, P, H, C and c1] and S, and between [N, P, H, C and c1] and G, described by the first principal component (Fig. 5F). The difference between S and G was extremely subtle. In either case, the null hypothesis of no phylogenetic signal cannot be rejected (*P*-values of 0.365 and 0.335, respectively).

For pPCAs generated based on the tree reconstructed with mitochondrial data, the percentage of variance explained by the first two axes was 56.66% for the dataset with landmarks and 37.33% for the dataset with semi-landmarks, as shown in the Supporting Information (Data S3 and S4). When the phylogenetic analysis of principal components was weighed based on data from the collapsed tree, the percentage of changes explained in morphology was 58.03% for the dataset with landmarks and 36.75% for the dataset with semi-landmarks (Data S3A and S4A). For morphometric pPCA-based distances obtained using landmarks and the original phylogeny, the associations were significant for all

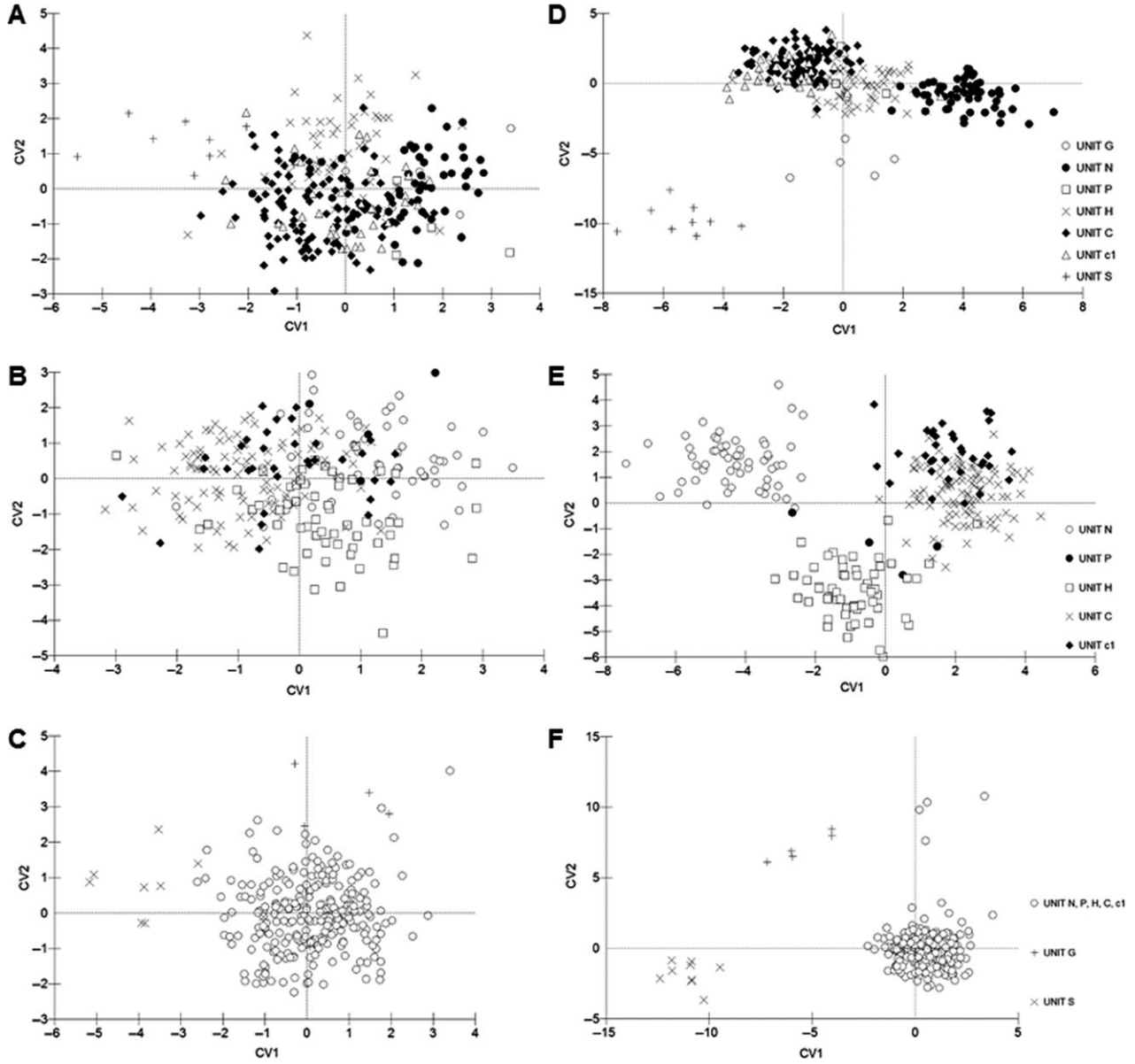

Figure 7. Scatterplots of canonical variate scores for the dataset with landmarks (A, B, C) and semi-landmarks (D, E, F) of the *Rhinella crucifer* group. In A and D, all categories are considered separately, in B and E only categories corresponding to closely related genetic units are considered, and in C and F closely related genetic units are considered as a single category.

variables, except for the variable annual precipitation and pPC1_semi (Table 4). Using the collapsed phylogeny, morphometric pPCA-based distances were associated with altitude, annual mean temperature, temperature annual range, annual precipitation, precipitation of the wettest month and precipitation of the wettest quarter, with the exception of pPC2, which was not significantly associated with annual precipitation (Table 4). For the pPCA with semi-landmarks, all the environmental variables were associated with the differences between morphological values with the exception of pPC2, which was not significantly associated with temperature annual range (Table 4).

DISCUSSION

HEAD SHAPE VARIATION IN THE *RHINELLA CRUCIFER* GROUP

From the ordination of scores of the analysed specimens, it is evident that the proportion of the total

Table 2. Probabilities of permutation tests for differences among groups as estimated by canonical variate analysis of Procrustes-fitted landmark data for genetic units of *Rhinella crucifer* group specimens used in this study

	Mahalanobis distance						Procrustes distance					
	c1	N	G	S	C	P	c1	N	G	S	C	P
(a)												
N	**<0.0001**						**0.0069**					
G	**0.0005**	0.0834					0.0890	0.3013				
S	**<0.0001**	**<0.0001**	**0.0003**				**0.0179**	**<0.0001**	**0.0038**			
C	**0.0160**	**<0.0001**	**0.0275**	**<0.0001**			0.3131	**0.0001**	0.0666	**0.0145**		
P	**0.0059**	**0.0024**	0.2443	**00.0005**	**0.0385**		0.0944	**0.0119**	0.0778	**0.0016**	**0.0343**	
H	**<0.0001**	**<0.0001**	**0.0127**	**<0.0001**	**<0.0001**	**0.0122**	**0.0085**	**0.0050**	0.3048	**0.0027**	**<0.0001**	**0.0084**
	G	S	C,c1,N,H				G	S	C,c1,N,H			
S	**0.0004**						**0.0052**					
C,c1,N,H, P	**0.0356**	**<0.0001**					0.1979	**0.0048**				
	c1	**N**	**C**	**P**			**c1**	**N**	**C**	**P**		
N	**0.0001**						**0.0146**					
C	**0.0169**	**<0.0001**					0.3388	**<0.0001**				
P	**0.0070**	**0.0024**	**0.0364**				0.0919	**0.0116**	**0.0345**			
H	**<0.0001**	**<0.0001**	**<0.0001**	**0.0090**			**0.0139**	**0.0049**	**<0.0001**	**0.0071**		
(b)												
N	**<0.0001**						**<0.0001**					
G	**<0.0001**	**<0.0001**					**0.0014**	0.1673				
S	**<0.0001**	**<0.0001**	**0.0001**				**0.0001**	**0.0001**	**0.0005**			
C	**<0.0001**	**<0.0001**	**<0.0001**	**<0.0001**			0.2055	**0.0011**	0.1075	**0.0067**		
P	**<0.0001**	**<0.0001**	**0.0031**	**0.0008**	**<0.0001**		**0.0005**	0.1115	0.0604	**<0.0001**	0.0734	
H	**<0.0001**	**<0.0001**	**<0.0001**	**<0.0001**	**<0.0001**	**<0.0001**	**0.0036**	**<0.0001**	0.0870	**0.0022**	**0.0091**	**0.0317**
	G	S	C,c1,N,H				G	S	C,c1,N,H			
S	**0.0002**						**0.0004**					
C,c1,N,H,P	**<0.0001**	**<0.0001**					0.1100	**0.0055**				
	c1	**N**	**C**	**P**			**c1**	**N**	**C**	**P**		
N	**<0.0001**						**0.0003**					
C	**<0.0001**	**<0.0001**					0.2014	**0.0031**				
P	**<0.0001**	**<0.0001**	**<0.0001**				**0.0008**	0.1174	0.0761			
H	**<0.0001**	**<0.0001**	**<0.0001**	**<0.0001**			**0.0035**	**<0.0001**	**0.0106**	**0.0354**		

P values < 0.005 are in bold type. (a) Dataset with landmarks; (b) dataset with semi-landmarks.

shape variation that is explained by the principal components is limited. This may be due to the recent diversification of the group (Thomé *et al.*, 2010), the typical conservatism in the skull of bufonids (Martin, 1972; Pramuk, 2006), the method used, which may have been inefficient in recovering shape patterns in these animals, or a combination of the three. Nonetheless, shape changes are detectable and related to specific structures in the head of specimens, as shown in the deformation grids. Analysis of landmark data revealed that specimens from the different genetic units differ in the shape of the cephalic crests and eye, relative to a consensus configuration. Analysis of semi-landmarks also showed changes in the shape of the parotoid gland, eye and contour of the mandibular arch. Note that Baldissera *et al.* (2004) used variation in the same structures qualitatively as taxonomic characters to differentiate among species in the group. This is not surprising because species in Baldissera *et al.* (2004) and the categories considered in the present paper show considerable overlap (see discussion in Thomé *et al.*, 2012). Furthermore, it highlights the ability of trained taxonomists to perceive subtle morphological variation despite the lack of guidance from genetic markers.

Table 3. Tree lengths computed with squared-change parsimony and *P* values for the permutation tests of phylogenetic signal (* = statistically significant value)

Phylogeny	Landmarks Tree length, *P*	Semi-landmarks Tree length, *P*
Mitochondrial tree	0.00631, 0.282	0.00702, 0.365
Collapsed tree	0.00325, <0.0001*	0.00351, 0.335

In the analyses including prior information (CVAs), the proportion of the variation among categories accommodated by the first canonical variates was usually large, being larger for landmarks than for semi-landmarks. Conversely, the biplots showed more definition in the separation of categories when the semi-landmarks were used. Both landmarks and semi-landmarks showed a similar pattern in terms of the amount of variation accommodated by the first two canonical variates in the different comparisons: the percentage of variation accommodated was larger in the comparisons in which we clustered the closest genetic units as a single category. This might be due to the fact that category H, representing specimens from the transition zone between N and C, is not a natural group and may include specimens belonging to each of these two genetic units and hybrids with transitional characteristics. Therefore, it is expected that analyses allowing for the comparison of this category with categories N and C would show a lack of discrimination.

Overall, our analyses indicate that there is size-free variation in the shape of the head of specimens in the *Rhinella crucifer* group, and that morphological changes are associated with specific structures. Variation is subtle, but sufficient to statistically differentiate among genetically defined units in most cases. The difference in number of analysed specimens among groups may be the cause of statistical discrepancies in significance in each comparison, as shown by Pillar (1999). In other words, the variation in sample size, in particular, affects the probability of committing type II statistical error.

Morphological analyses of single structures may be difficult. In the work of Clemente-Carvalho *et al.* (2011), some variant patterns in morphology were not detected with the use of landmarks alone. In

Table 4. Results of Mantel tests for association between morphological differentiations across specimens of the species of the *Rhinella crucifer* group vs. six environmental distance variables (see text for details)

	Explanatory variable					
Dependent variable	Elevation	AnnMTemp	TempAnnRge	AnnPrec	PrecWetMon	PrecWetQtr
pPC1#12_full mitochondrial tree	0.001*	0.03*	0.03*	0.006*	0.01*	0.006*
pPC2#12_ full mitochondrial tree	0.004*	0.01*	0.04*	0.0001*	0.03*	0.02*
pPC1#semi_ full mitochondrial tree	0.02*	0.006*	0.03*	n.s.	0.01*	0.001*
pPC2#semi_ full mitochondrial tree	0.01*	0.009*	0.006*	0.04*	0.02*	0.006*
pPC1#12_collapsed	0.02*	0.01*	0.02*	0.01*	0.01*	0.005*
pPC2#12_collapsed	0.02*	0.03*	0.03*	n.s.	0.009*	0.01*
pPC1#semi_collapsed	0.003*	0.01*	0.02*	0.02*	0.03*	0.03*
pPC2#semi_collapsed	0.007*	0.01*	n.s.	0.0008*	0.003*	0.009*

Dependent variables are the first two axes from pPCA (for both datasets). Mantel correlation values are given where significant (*$P < 0.005$; n.s., not significant).

particular, landmark-based geometric morphometric approaches may be insufficient for analysing structures without clear points of homology. In such cases, the addition of semi-landmarks may provide new information on curves and surfaces, allowing for better descriptions and finer analysis of the complexity of biological form (Gunz, Mitteroecker & Bookstein, 2005; Perez, Bernal & Gonzalez, 2006; Gunz *et al.*, 2009). In our analyses, landmarks and semi-landmarks highlighted shape changes associated with different structures, showing that the analyses of both types of data are complementary in portraying the geographical nature of morphological differentiation.

Shape is partially explained by genetic relatedness

Phylogenetic signal is defined as the degree to which phylogenetic relatedness among taxa is associated with their phenotypic similarity (e.g. Blomberg, Garland & Ives, 2003; Cardini & Elton, 2008). Therefore, if closely related taxa are morphologically more similar than more distant taxa, phylogenetic signal may be detected. We first approached this by conducting CVA hierarchically. Analyses comparing all genetic categories accommodated less variation than analyses in which we clustered the most closely related categories, as one would expect in the presence of phylogenetic signal (although fewer groups result in fewer CVs, which may cause higher variation in the first CV). Also, the biplots show more proximity (and overlaps) of the categories N, P, C, c1 and H, whereas categories G and S are confined to more peripheral regions of the multivariate space. Category c1 represents a haplogroup within genetic unit C whose geographical distribution is somewhat concordant with the distribution of *Rhinella abei*, a species described by Baldissera *et al.* (2004) using morphological criteria. This species was not detected in the multilocus analyses of Thomé *et al.* (2012) and its recognition under a phylogenetic species concept is pending more genetic markers. It is impossible, however, to confirm that the overlap between the scores of specimens from unit c1 and C indicates that this category has no biological meaning. Interestingly, Baldissera *et al.* (2004) obtained a similar pattern in their traditional morphometric analysis, with the scores of *R. abei* being nested within the polygon of *R. ornata*, here included as category C. For G and S, the most divergent genetic units in the group according to the mitochondrial DNA, interpretation of the results was more straightforward, as all biplots showed a trend of isolation of their respective scores. However, scores from P are also usually fairly isolated, even though genetic unit P is sister to C, denoting unexpected variation in shape for this genetic unit.

We applied a more rigorous test by mapping the principal components on a phylogeny. We then assessed statistical significance by simulating the hypothesis of no phylogenetic signal using permutations. We were able to detect the effect of relatedness with the landmark dataset, but only when considering the closest genetic units as one taxon, with the two remaining taxa showing more strongly defined shape changes as genetic divergence increased. It is possible that the lack of significance in the analysis based upon the original tree is caused by the morphological dissimilarity of P compared with all other units. The failure in rejecting the null hypothesis of no phylogenetic signal with the semi-landmark dataset is intriguing, as these seem to graphically provide better-defined results in the CVAs (Fig. 7). Taking all the results together, it is only possible to confirm that the evolutionary history of the group explains the variation in the shape of the head to a limited extent.

Influence of physical environment

The geographical distribution of species or groups of closely related species may be broad enough that various characteristics of their environment vary within their range (e.g. Keller *et al.*, 2013). Phylogenetic comparative methods are often employed for studying the relationship between phenotypes and environment (*sensu* Gould & Vrba, 1982). These methods allow for the partitioning of phenotypic variation into phylogenetic (endogenous) and non-phylogenetic (exogenous) components (Levin, 1992; Levin & Pacala, 1997; Martins & Hansen, 1997; Felsenstein, 2003). However, the assumption that the exogenous component is always related to the physical environment can be equivocal (Polly *et al.*, 2013), making it necessary to determine the degree of direct influence of each variable on the changes in shape. Elucidation of the direct mechanism behind the influence of environment over development and, consequently, adult morphology is beyond the scope of our study. Nevertheless, we minimized a possible effect of relatedness (with the phylogenetic PCA) and tested for associations of local climates and elevation with shape because it has been suggested that morphology in anurans is particularly sensitive to environmental conditions (Marcelino *et al.*, 2009). A significant proportion of the variation in head morphology among particular species can be statistically explained by the majority of the environmental factors taken into account (see Table 3 for details). It suggests that variability in the physical environment constitutes an important factor in the determination

of head morphology and should be considered as a source of variation. More specifically, it appears that populations of the same genetic category living in the areas differing the most in environmental conditions display more dissimilar morphotypes, whereas individuals from different genetic categories occupying areas with similar environmental characteristics may display somewhat similar cranial shapes. Particularly, some individuals of N and C (and from C and c1) from regions geographically adjacent seem less distinguishable in morphospace (see Supporting Information for geographical origins of specimens). An equivalent response by different species to a shared environment, assuming that climate and elevation in geographically adjacent regions are probably similar, is the most plausible explanation for this morphological similarity. Alternatively, the efforts of Thomé *et al.* (2012) may have been insufficient to properly delimit the zone of putative hybridization between N and C, and the similarity between categories near the zone of contact of their ranges could be explained by interspecific hybridization and subsequent introgression of morphotype-mediated genes (*sensu* Grant & Grant, 2002). Although the correlation observed between body shape and environmental variables suggests an important role for environmental conditions in the production of morphological variation in these taxa, many interpretations of our results are possible. Future experimental work (e.g. common garden or reciprocal transplant experiments in conjunction with quantitative genetics) may identify the evolutionary and ecological processes responsible for the observed matching between the environment and morphology in examined species (Gvozdík *et al.*, 2008). Such experimental approaches could determine whether similar morphology is caused by a shared plastic responses to environmental conditions.

CONCLUSIONS

In this study we used geometric morphometrics to reassess morphometric variation in the *Rhinella crucifer* group and to consider its evolutionary history and local variation relative to environmental conditions (e.g. climate and altitude). Our main questions were: (1) Is there size-free shape variation in the group? (2) If so, can this variation be explained by genetic relatedness. (3) Is shape variation influenced by local variation of the physical environment? Our results revealed that there is size-free shape morphological variation in toads of the *Rhinella crucifer* group. Variation is subtle, but sufficient to differentiate among genetically defined units in most cases. Shape changes are related to specific structures in the head of specimens defined by landmarks and semi-landmarks, highlighting changes associated with different structures, showing that the analysis of both types of data is complementary. Variation can be explained both by genetic relatedness and by local physical environment. The effects of relatedness were first revealed by hierarchical CVA, where analyses comparing all categories accommodated less variation than analyses in which we clustered the most closely related categories. Also, biplots showed restriction of more divergent categories to peripheral regions of morphospace, whereas scores of other categories often overlapped. We were also able to statistically detect the effect of relatedness with landmark data when considering the closest genetic units as a single category. A significant share of the variation in head morphology of the group can be explained by environmental variables, suggesting that conditions of the physical environment should be considered as a source of morphological variation. Future experimental work may lead to a better understanding of the roles of physical variables, plasticity and relatedness as causes underlying morphological variation.

ACKNOWLEDGEMENTS

We are deeply grateful to the two anonymous reviewers for the careful evaluation of our manuscript. We thank F. Toledo, F. Brusquetti Estrada, H. Zaher and L. Nascimento for access to specimens under their care. We are grateful to S. dos Reis and R. Clemente-Carvalho for help in learning morphometry techniques and advice in their most diverse applications; C. Espana for help in obtaining the images at the beginning of this work; S. Bogão Marques de Sousa for help with logistics; and the Instituto Chico Mendes (ICMBio) for collecting and export permits (nos. 13110-1 and 103420). Funding was provided by grants #2005/52727-5, #2006/56938-3, #2007/521136-2, #2008/50928-1 and #2013/50741-7 by São Paulo Research Foundation (FAPESP), and C.F.B.H. was supported by a fellowship from the Conselho Nacional de Desenvolvimento Científico e Tecnológico.

REFERENCES

Adams DC, Rohlf FJ, Slice DE. 2004. Geometric morphometrics: ten years of progress following the 'revolution'. *Italian Journal of Zoology* **71:** 5–16.

Baldissera FA, Caramaschi U, Haddad CFB. 2004. Review of the *Bufo crucifer* species group, with descriptions of two new related species (Amphibia, Anura, Bufonidae). *Arquivos do Museu Nacional* **62:** 255–282.

Baylac M, Friess M. 2005. Fourier descriptors, Procrustes superimposition, and data dimensionality: an example of cranial shape analysis in modern human populations. In: Slice EE, ed. *Modern morphometrics in physical*

antropology. New York: Kluwer Academic/Plenum Publishers, 145–165.

Blomberg SP, Garland T Jr, Ives AR. 2003. Testing for phylogenetic signal in comparative data: behavioral traits are more labile. *Evolution* **57:** 717–745.

Bookstein FL. 1991. *Morphometric tools for landmark data: geometry and biology*. Cambridge, UK: Cambridge University Press.

Bookstein FL. 1996. Biometrics, biomathematics, and the morphometrics synthesis. *Bulletin of Mathematical Biology* **58:** 313–365.

Bookstein FL. 1997. Landmark methods for forms without landmarks: localizing group differences in outline shape. *Medical Image Analysis* **1:** 225–243.

Bookstein FL, Streissguth AP, Sampson PD, Connor PD, Barr HM. 2002. Corpus callosum shape and neuropsychological deficits in adult males with heavy fetal alcohol exposure. *NeuroImage* **15:** 233–251.

Cardini A, Elton S. 2008. Does the skull carry a phylogenetic signal? Evolution and modularity in the guenons. *Biological Journal of the Linnean Society* **93:** 813–834.

Castellano S, Giacoma C. 1998. Morphological variation of the green toad, *Bufo viridis*, in Italy: a test of causation. *Journal of Herpetology* **32:** 540–550.

Castellano S, Rosso A, Doglio S, Giacoma C. 1999. Body size and calling variation in the green toad (*Bufo viridis*). *Journal of Zoology* **248:** 83–90.

Clemente-Carvalho RBG, Monteiro LR, Bonato V, Rocha HS, Pereira GR, Oliveira DS, Lopes TR, Haddad CFB, Martins EG, Dos Reis SF. 2008. Geographic variation in cranial shape in the pumpkin toadlet (*Brachycephalus ephippium*): a geometric analysis. *Journal of Herpetology* **42:** 176–185.

Clemente-Carvalho RBG, Alves ACR, Perez SI, Haddad CFB, Dos Reis SF. 2011. Morphological and molecular variation in the pumpkin toadlet, *Brachycephalus ephippium* (Anura: Brachycephalidae). *Journal of Herpetology* **45:** 94–99.

Cole TM III, Lele SR, Richtsmeier JT. 2002. A parametric bootstrap approach to the detection of phylogenetic signal in landmark data. In: MacLeod N, Forey PL, eds. *Morpholgy, shape and phylogeny*. London: Taylor and Francis, 194–219.

Croix SL, Holekamp KE, Shivik JA, Lundrigan BL, Zelditch ML. 2011. Ontogenetic relationships between cranium and mandible in coyotes and hyenas. *Journal of Morphology* **272:** 662–674.

Dryden IL, Mardia KV. 1998. *Statistical shape analysis*. New York: John Wiley and Sons.

Felsenstein J. 2003. *Inferring phylogenies*. Sunderland, MA: Sinauer Associates.

Frost DR. 2014. *Amphibian species of the world: an online reference*. Version 5.5 (16 March, 2011). Available at http://research.amnh.org/vz/herpetology/amphibia/. American Museum of Natural History, New York.

Goodall C. 1991. Procrustes methods in the statistical analysis of shape. *Journal of the Royal Statistical Society (Series B)* **53:** 285–339.

Goslee SC, Urban DL. 2007. The ecodist package for dissimilarity-based analysis of ecological data. *Journal of Statistical Software* **22:** 1–19.

Gould SJ, Johnston RF. 1972. Geographic variation. *Annual Review of Ecology and Systematics* **3:** 457–498.

Gould SJ, Vrba ES. 1982. Expatation – a missing term in the science of form. *Paleobiology* **8:** 4–15.

Grant PR, Grant BR. 2002. Unpredictable evolution in a 30-year study of Darwin's finches. *Science* **296:** 707–711.

Gunz P, Mitteroecker P, Bookstein FL. 2005. Semilandmarks in three dimensions. In: Slice DE, ed. *Modern morphometrics in physical anthropology*. New York: Kluwer Academic/Plenum Publishers, 73–98.

Gunz P, Bookstein FL, Mitteroecker P, Stadlmayr A, Seidler H, Weber GW. 2009. Early modern human diversity suggests subdivided population structure and a complex out-of-Africa scenario. *Proceedings of the National Academy of Sciences of the United States of America* **106:** 6094–6098.

Gvozdík V, Moravec J, Kratochvíl L. 2008. Geographic morphological variation in parapatric western Palearctic tree frog, *Hyla arborea* and *Hyla savignyi*: are related species similarly affected by climatic conditions? *Biological Journal of Linnean Society* **95:** 539–556.

Haddad CFB, Toledo LF, Prado CPA, Loebmann D, Gasparini JL, Sazima I. 2013. *Guia de anfíbios da mata atlântica – diversidade e biologia*. São Paulo, SP: Anolis Books.

Hijmans RJ, Cameron SE, Parra JL, Jones PG, Jarvis A. 2005. Very high resolution interpolated climate surfaces for global land areas. *International Journal of Climatology* **25:** 1965–1978.

Ivanović A, Sotiropoulos K, Vukov TD, Eleftherakos K, Dzukić G, Polymeni RM, Kalezić ML. 2008. Cranial shape variation and molecular phylogenetic structure of crested newts (*Triturus cristatus* superspecies: Caudata, Salamandridae) in the Balkans. *Biological Journal of the Linnean Society* **95:** 348–360.

Ivanović A, Sotiropoulos K, Dzukić G, Kalezić ML. 2009. Skull size and shape variation versus molecular phylogeny: a case study of alpine newts (*Mesotriton alpestris*, Salamandridae) from the Balkan Peninsula. *Zoomorphology* **128:** 157–167.

Ivanović A, Sotiropoulos K, Uzum N, Dzukić G, Olgun K, Cogălniceanu D, Kalezić ML. 2011. A phylogenetic view on skull and shape variation in the smooth newt (*Lissotriton vulgaris*, Caudata, Salamandridae). *Journal of Zoological Systematics and Revolutionary Research* **50:** 116–124.

Keller I, Alexander JM, Holderegger R, Edwars PJ. 2013. Widespread phenotypic and genetic divergence along altitudinal gradients in animals. *Journal of Evolutionary Biology* **26:** 2527–2543.

Klingenberg CP. 2011. MorphoJ: an integrated software package for geometric morphometrics. *Molecular Ecology Resources* **11:** 353–357.

Klingenberg CP. 2013. Visualizations in geometric morphometrics: how to read and how to make graphs showing

shape changes. *Hystrix, The Italian Journal of Mammalogy* **24:** 15–24.

Klingenberg CP, Gidaszewski NA. 2010. Testing and quantifying phylogenetic signals and homoplasy in morphometric data. *Systematic Biology* **59:** 245–261.

Klingenberg CP, Monteiro LR. 2005. Distances and directions in multidimensional shape spaces: implications for morphometric applications. *Systematic Biology* **54:** 678–688.

Kutrup B, Bulbul U, Yilmaz N. 2006. Effects of the ecological conditions on morphological variations of the Green toad, *Bufo viridis*, in Turkey. *Ecological Research* **21:** 208–214.

Levin SA. 1992. The problem of scale in ecology. *Ecology* **73:** 1943–1967.

Levin SA, Pacala SW. 1997. Theories of simplification and scaling of spatially distributed process. In: Tilman D, Kareiva P, eds. *Space ecology: the role of space in population dynamics and interspecific interactions*. Princeton, NJ: Princeton University Press, 271–295.

Lima AMX, Rodrigues RG, Bittencourt S, Condrati LH, Machado RA. 2005. *Bufo henseli*. First record. *Herpetological Review* **36:** 198.

Lutz A. 1934. Notas subre especies brasileiras do genero *Bufo*/Zur Kenntnis der Brasilianischen Kroeten vom Genus *Bufo*. *Memórias do Instituto Oswaldo Cruz* Rio de Janeiro **28:** 111–134.

MacLeod N. 2002. Phylogenetic signal in morphometric data. In: MacLeod N, Forey PL, eds. *Morpholgy, shape and phylogeny*. London: Taylor and Francis, 100–138.

Maddison WP. 1991. Squared–change parsimony reconstructions of ancestral states for continuous–valued characters on a phylogenetic tree. *Systematic Zoology* **40:** 304–314.

Marcelino VR, Haddad CFB, Alexandrino JMB. 2009. Geographic distribution and morphological variation of striped and nostriped populations of the Brazilian Atlantic forest treefrog *Hypsiboas bischoffi* (Anura: Hylidae). *Journal of Herpetology* **42:** 351–361.

Martin RF. 1972. Osteology and evolution in Neotropical *Bufo*. *American Midland Naturalist* **88:** 301–317.

Martins EP, Hansen TF. 1997. Phylogenies and the comparative method: a general approach to incorporating phylogenetic information into analysis of interspecific data. *The American Naturalist* **149:**646–667.

McArdle BH, Rodrigo AG. 1994. Estimating the ancestral atates of a continuous-valued character using squared-change parsimony: an analytical solution. *Systematic Biology* **43:** 573–578.

Mitteroecker P, Gunz P. 2009. Advances in geometric morphometrics. *Evolutionary Biology* **36:** 235–247.

Oxnard CE. 1978. One biologist's view of morphometrics. *Annual Review of Ecology and Systematics* **9:** 219–241.

Paradis E, Claude J, Strimmer K. 2004. APE: analysis of phylogenetics and evolution in R. *Bioinformatics* **2:** 289–290.

Perez SI, Bernal V, Gonzalez P. 2006. Differences between sliding semi-landmarks methods: implications for shape analyses of human populations. *Journal of Anatomy* **208:** 769–784.

Pillar VD. 1999. The bootstrapped ordination re-examined. *Journal of Vegetation Science* **10:** 895–902.

Polly PD, Lawing AM, Fabre A, Goswami A. 2013. Phylogenetic principal components analysis and geometric morphometrics. *Hystrix, The Italian Journal of Mammalogy* **24:** 1–9.

Pramuk JB. 2006. Phylogeny of South American *Bufo* (Anura: Bufonidae) inferred from combined evidence. *Zoological Journal of the Linnean Society* **146:** 407–452.

R Development Core Team. 2014. *R: a language and environment for statistical computing*. Vienna: R Foundation for Statistical Computing.

Revell LJ. 2009. Size-correction and principal components for interspecific comparative studies. *Evolution* **63–12:** 3258–3268.

Revell LJ. 2012. phytools: an R package for phylogenetic comparative biology (and other things). *Method in Ecology and Evolution* **3:** 217–223.

Roberto IJ, Brito L, Thomé MTC. 2014. A new species of *Rhinella* (Anura: Bufonidae) from Northeastern of Brazil. *South America Journal of Herpetology* **9:** 190–199.

Rohlf FJ. 1993. Relative warp analysis and an example of its application to mosquito wings. In: Marcus LF, Garcia-Valdecasas AE, eds. *Contributions to morphometrics*, Vol. 8. Madrid: Museo Nacional de Ciencias Naturales (CSIC), 131–159.

Rohlf FJ. 2001. Comparative methods for the analysis of continuous variables: geometric interpretations. *Evolution* **55:** 2143–2160.

Rohlf FJ. 2004. *tps serie softwares*. Available at http// life.bio.sunysb.edu/morph/.

Rohlf FJ. 2005. *tpsDIG 2.10*. Stony Brook, NY: SUNY. Available at: http://life.bio.sunysb.edu/morph.

Rohlf FJ, Loy A, Corti M. 1996. Morphometric analysis of Old World Talpidae (Mammalia, Insectivora) using partial-warp scores. *Systematic Biology* **45:** 344–362.

Rosso A, Castellano S, Giacoma C. 2004. Ecogeography analysis of morphological and life-history variation in the Italian treefrog. *Evolutionary Ecology* **18:** 303–321.

Sampson PD, Bookstein FL, Sheehan H, Bolson EL. 1996. Eigenshape analysis of left ventricular outlines from contrast ventriculograms. In: Marcus LF, Corti M, Loy A, Naylor GJP, Slice DE, eds. *Advances in morphometrics*, Vol. 284. Nato ASI Series, Series A: Life Science. New York: Plenum, 131–152.

Schauble C. 2004. Variation in the body size and sexual dimorphism across geographical and environmental space in the frogs *Limnodynastes tasmaniensis* and *L. peronii*. *Biological Journal of the Linnean Society* **82:** 39–56.

Sheets HD, Keonho K, Mitchell CE. 2004. A combined landmark and outline-based approach to ontogenetic shape change in the Ordovician trilobite *Triarthrus becki*. In: Elewa A, ed. *Applications of morphometrics in paleontology and biology*. New York: Springer, 67–81.

Silveira AL, Salles ROL, Pontes RC. 2009. Primeiro registro de *Rhinella pombali* e novos registros de *R. crucifer* e *R. ornata* no Estado do Rio de Janeiro, Brasil (Amphibia, Anura, Bufonidae). *Biotemas* **22:** 231–235.

Smouse PE, Long JC, Sokal RR. 1986. Multiple regression and correlation extensions of the Mantel test of matrix correspondence. *Systematic Zoology* **35:** 627–632.

Spix JB. 1824. Animalia nova sive Species novae *Testudinum et Ranarum* quas in itinere per Brasilian annis MDCCCXVII – MDCCCXX jussu et auspiciis Maximiliani Josephi I. Bavariae Regis. Munchen: F. S. Hubschmann.

Thomé MTC, Zamudio KR, Giovanelli JGR, Haddad CFB, Baldissera FA Jr, Alexandrino J. 2010. Phylogeography of endemic toads and post-Pliocene persistence of the Brazilian Atlantic forest. *Molecular Phylogenetics and Evolution* **55:** 1018–1031.

Thomé MTC, Zamudio KR, Haddad CFB, Alexandrino J. 2012. Delimiting genetic units in Neotropical toads under incomplete lineage sorting and hybridization. *BMC Evolutionary Biology* **12:** 242.

Turchetto-Zolet AC, Pinheiro F, Salgueiro F, Palma-Silva C. 2013. Phylogeographical patterns shed light on evolutionary process in South America. *Molecular Ecology* **12:** 1193–1213.

Vaz-Silva W, Valdujo PH, Pombal JP Jr. 2012. New species of the *Rhinella crucifer* group (Anura, Bufonidae) from the Brazilian Cerrado. *Zootaxa* **3265:** 57–65.

Vieira KS, Arzabe C, Hernandez MIM, Vieira WLS. 2008. An examination of morphometric variations in a Neotropical toad population (*Proceratophrys cristiceps*, Amphibia, Anura, Cycloramphidae). *PLoS ONE* **3:** e3934.

Wied-Neuwied MA. 1821. *Reise nach Brasilien in den Jaheren 1815 bis 1817*, vol. 2. Frankfurt a. M.: Henrich Ludwig Bronner.

SUPPORTING INFORMATION

Additional supporting information may be found online in the supporting information tab for this article:

Data S1. Probabilities of the regression obtained by permutation tests.
Data S2. Positioning of scores in multidimensional space represented by the first two principal components.
Data S3. Positioning of scores in multidimensional space represented by the first two phylogenetic principal components for the data set with only landmarks.
Data S4. Positioning of scores in multidimensional space represented by the first two phylogenetic principal components for the data set with only semilandmarks.
Data S5. Scores of the canonical variation and geographic origins for each specimen considered in the study.

APPENDIX 1

Representative specimens of all species of the *Rhinella crucifer* group analysed in this study. CFBH, 'Célio F. B. Haddad' amphibian collection; IIBPH, herpetological collection of the 'Instituto de Investigación Biológica del Paraguay'; MZUSP, Museum of Zoology University of São Paulo; MCNPUC, Museum of Natural Sciences of the Pontifícia Universidade Católica de Minas Gerais).

Collection no.	Species	Unit	Municipality	State/Country	Locality	Latitude	Longitude
CFBH_118	*Rhinella ornata*	C	Ubatuba	SP/BR	L1	−23.3433861	−45.085710
CFBH_1206	*Rhinella ornata*	C	Ubatuba	SP/BR	L1	−23.3433861	−45.085710
CFBH_1208	*Rhinella ornata*	C	Ubatuba	SP/BR	L1	−23.3433861	−45.085710
CFBH_1210	*Rhinella ornata*	C	Ubatuba	SP/BR	L1	−23.3433861	−45.085710
CFBH_1216	*Rhinella ornata*	C	Ubatuba	SP/BR	L1	−23.3433861	−45.085710
CFBH_1218	*Rhinella ornata*	C	Ubatuba	SP/BR	L1	−23.3433861	−45.085710
CFBH_1219	*Rhinella ornata*	C	Ubatuba	SP/BR	L1	−23.3433861	−45.085710
CFBH_1220	*Rhinella ornata*	C	Ubatuba	SP/BR	L1	−23.3433861	−45.085710
CFBH_12545	*Rhinella ornata*	C	Ubatuba	SP/BR	L1	−23.3433861	−45.085710
CFBH_12547	*Rhinella ornata*	C	Ubatuba	SP/BR	L1	−23.3433861	−45.085710
CFBH_12549	*Rhinella ornata*	C	Ubatuba	SP/BR	L1	−23.3433861	−45.085710
CFBH_12551	*Rhinella ornata*	C	Ubatuba	SP/BR	L1	−23.3433861	−45.085710
CFBH_12552	*Rhinella ornata*	C	Ubatuba	SP/BR	L1	−23.3433861	−45.085710
CFBH_12553	*Rhinella ornata*	C	Ubatuba	SP/BR	L1	−23.3433861	−45.085710
CFBH_12554	*Rhinella ornata*	C	Ubatuba	SP/BR	L1	−23.3433861	−45.085710
CFBH_12558	*Rhinella ornata*	C	Ubatuba	SP/BR	L1	−23.3433861	−45.085710
CFBH_12559	*Rhinella ornata*	C	Ubatuba	SP/BR	L1	−23.3433861	−45.085710
CFBH_12563	*Rhinella ornata*	C	Ubatuba	SP/BR	L1	−23.3433861	−45.085710

Appendix 1. *Continued*

Collection no.	Species	Unit	Municipality	State/Country	Locality	Latitude	Longitude
CFBH_12564	*Rhinella ornata*	C	Ubatuba	SP/BR	L1	−23.3433861	−45.085710
CFBH_13361	*Rhinella crucifer*	N	Caraíva	BA/BR	L2	−16.800000	−39.150000
CFBH_13363	*Rhinella crucifer*	N	Caraíva	BA/BR	L2	−16.800000	−39.150000
CFBH_13364	*Rhinella crucifer*	N	Caraíva	BA/BR	L2	−16.800000	−39.150000
CFBH_13365	*Rhinella crucifer*	N	Caraíva	BA/BR	L2	−16.800000	−39.150000
CFBH_13366	*Rhinella crucifer*	N	Caraíva	BA/BR	L2	−16.800000	−39.150000
CFBH_13367	*Rhinella crucifer*	N	Caraíva	BA/BR	L2	−16.800000	−39.150000
CFBH_13368	*Rhinella crucifer*	N	Caraíva	BA/BR	L2	−16.800000	−39.150000
CFBH_13370	*Rhinella crucifer*	N	Caraíva	BA/BR	L2	−16.800000	−39.150000
CFBH_13371	*Rhinella crucifer*	N	Caraíva	BA/BR	L2	−16.800000	−39.150000
CFBH_13372	*Rhinella crucifer*	N	Caraíva	BA/BR	L2	−16.800000	−39.150000
CFBH_13374	*Rhinella crucifer*	N	Caraíva	BA/BR	L2	−16.800000	−39.150000
CFBH_13399	*Rhinella crucifer*	N	Caraíva	BA/BR	L2	−16.800000	−39.150000
CFBH_1373	*Rhinella ornata*	C	Rio Claro	SP/BR	L3	−22.413399	−47.569574
CFBH_1377	*Rhinella crucifer*	H	Parati	RJ/BR	L4	−23.216708	−44.717938
CFBH_13938	*Rhinella ornata*	H	Petrópolis	RJ/BR	L5	−22.504639	−43.182329
CFBH_14647	Putative hybrid	C	Cristina	MG/BR	L6	−22.209178	−45.271985
CFBH_14812	*Rhinella ornata*	C	São Luís do Paraitinga	SP/BR	L7	−23.228066	−45.322663
CFBH_15345	*Rhinella ornata*	C	Ilha Bela	SP/BR	L8	−23.904000	−45.335000
CFBH_15349	*Rhinella ornata*	C	Ilha Bela	SP/BR	L8	−23.904000	−45.335000
CFBH_15351	*Rhinella ornata*	C	Ilha Bela	SP/BR	L8	−23.904000	−45.335000
CFBH_15352	*Rhinella ornata*	C	Ilha Bela	SP/BR	L8	−23.904000	−45.335000
CFBH_15353	*Rhinella ornata*	C	Ilha Bela	SP/BR	L8	−23.904000	−45.335000
CFBH_15354	*Rhinella ornata*	C	Ilha Bela	SP/BR	L8	−23.904000	−45.335000
CFBH_15356	*Rhinella ornata*	C	Ilha Bela	SP/BR	L8	−23.904000	−45.335000
CFBH_15358	*Rhinella ornata*	C	Ilha Bela	SP/BR	L8	−23.904000	−45.335000
CFBH_15359	*Rhinella ornata*	C	Ilha Bela	SP/BR	L8	−23.904000	−45.335000
CFBH_15360	*Rhinella ornata*	C	Ilha Bela	SP/BR	L8	−23.904000	−45.335000
CFBH_15361	*Rhinella ornata*	C	Ilha Bela	SP/BR	L8	−23.904000	−45.335000
CFBH_15362	*Rhinella ornata*	C	Ilha Bela	SP/BR	L8	−23.904000	−45.335000
CFBH_15363	*Rhinella ornata*	C	Ilha Bela	SP/BR	L8	−23.904000	−45.335000
CFBH_15364	*Rhinella ornata*	C	Ilha Bela	SP/BR	L8	−23.904000	−45.335000
CFBH_15365	*Rhinella ornata*	C	Ilha Bela	SP/BR	L8	−23.904000	−45.335000
CFBH_15366	*Rhinella ornata*	C	Ilha Bela	SP/BR	L8	−23.904000	−45.335000
CFBH_15368	*Rhinella ornata*	C	Ilha Bela	SP/BR	L8	−23.904000	−45.335000
CFBH_15369	*Rhinella ornata*	C	Ilha Bela	SP/BR	L8	−23.904000	−45.335000
CFBH_15379	*Rhinella ornata*	C	Ilha Bela	SP/BR	L8	−23.904000	−45.335000
CFBH_15383	*Rhinella ornata*	C	Ilha Bela	SP/BR	L8	−23.904000	−45.335000
CFBH_15385	*Rhinella ornata*	C	Ilha Bela	SP/BR	L8	−23.904000	−45.335000
CFBH_15386	*Rhinella ornata*	C	Ilha Bela	SP/BR	L8	−23.904000	−45.335000
CFBH_15390	*Rhinella ornata*	C	Ilha Bela	SP/BR	L8	−23.904000	−45.335000
CFBH_16310	*Rhinella ornata*	C	São Luís do Paraitinga	SP/BR	L7	−23.228066	−45.322663
CFBH_16311	*Rhinella ornata*	C	São Luís do Paraitinga	SP/BR	L7	−23.228066	−45.322663
CFBH_16518	*Rhinella ornata*	C	Ubatuba	SP/BR	L1	−23.3433861	−45.085710
CFBH_1683	*Rhinella ornata*	C	Ubatuba	SP/BR	L1	−23.3433861	−45.085710
CFBH_1689	*Rhinella ornata*	C	Capão Bonito	SP/BR	L9	−24.003998	−48.339266
CFBH_17400	*Rhinella ornata*	C	Ilha Bela	SP/BR	L8	−23.904000	−45.335000
CFBH_1748	*Rhinella ornata*	C	Ubatuba	SP/BR	L1	−23.3433861	−45.085710
CFBH_1749	*Rhinella ornata*	C	Ubatuba	SP/BR	L1	−23.3433861	−45.085710
CFBH_1750	*Rhinella ornata*	C	Ubatuba	SP/BR	L1	−23.3433861	−45.085710

Appendix 1. *Continued*

Collection no.	Species	Unit	Municipality	State/Country	Locality	Latitude	Longitude
CFBH_18001	*Rhinella crucifer*	H	Santa Leopoldina	ES/BR	L10	−20.102515	−40.529283
CFBH_18090	*Rhinella crucifer*	H	Linhares	ES/BR	L11	−19.390915	−40.071503
CFBH_18091	*Rhinella crucifer*	H	Linhares	ES/BR	L11	−19.390915	−40.071503
CFBH_18141	*Rhinella abei*	c1	Quatro Barras	PR/BR	L12	−25.367153	−49.074947
CFBH_18163	*Rhinella abei*	c1	Blumenau	SC/BR	L13	−26.918996	−49.066078
CFBH_18164	*Rhinella abei*	c1	Blumenau	SC/BR	L13	−26.918996	−49.066078
CFBH_18166	*Rhinella abei*	c1	Blumenau	SC/BR	L13	−26.918996	−49.066078
CFBH_18168	*Rhinella abei*	c1	Blumenau	SC/BR	L13	−26.918996	−49.066078
CFBH_18169	*Rhinella abei*	c1	Blumenau	SC/BR	L13	−26.918996	−49.066078
CFBH_18175	*Rhinella abei*	c1	Massaranduba	SC/BR	L14	−26.610913	−49.009150
CFBH_18176	*Rhinella abei*	c1	Massaranduba	SC/BR	L14	−26.610913	−49.009150
CFBH_18177	*Rhinella abei*	c1	Massaranduba	SC/BR	L14	−26.610913	−49.009150
CFBH_18178	*Rhinella abei*	c1	Massaranduba	SC/BR	L14	−26.610913	−49.009150
CFBH_18179	*Rhinella abei*	c1	Massaranduba	SC/BR	L14	−26.610913	−49.009150
CFBH_18180	*Rhinella abei*	c1	Massaranduba	SC/BR	L14	−26.610913	−49.009150
CFBH_18181	*Rhinella abei*	c1	Massaranduba	SC/BR	L14	−26.610913	−49.009150
CFBH_18182	*Rhinella abei*	c1	Massaranduba	SC/BR	L14	−26.610913	−49.009150
CFBH_18238	*Rhinella henseli*	S	Bento Goncalves	RS/BR	L15	−29.096543	−51.451038
CFBH_18382	*Rhinella ornata*	C	Teodoro Sampaio	SP/BR	L16	−22.531624	−52.183277
CFBH_18387	*Rhinella ornata*	C	Teodoro Sampaio	SP/BR	L16	−22.531624	−52.183277
CFBH_18717	*Rhinella crucifer*	N	Aurelino Leal	BA/BR	L17	−14.360787	−39.408552
CFBH_18815	*Rhinella crucifer*	H	Teresópolis	RJ/BR	L18	−22.412324	−42.966432
CFBH_18816	*Rhinella crucifer*	H	Teresópolis	RJ/BR	L18	−22.412324	−42.966432
CFBH_20277	*Rhinella henseli*	S	Anitápolis	SC/BR	L19	−27.902458	−49.129065
CFBH_20278	*Rhinella henseli*	S	Anitápolis	SC/BR	L19	−27.902458	−49.129065
CFBH_20279	*Rhinella henseli*	S	Anitápolis	SC/BR	L19	−27.902458	−49.129065
CFBH_20280	*Rhinella henseli*	S	Anitápolis	SC/BR	L19	−27.902458	−49.129065
CFBH_20281	*Rhinella henseli*	S	Anitápolis	SC/BR	L19	−27.902458	−49.129065
CFBH_20282	*Rhinella abei*	c1	Anitápolis	SC/BR	L19	−27.902458	−49.129065
CFBH_20283	*Rhinella abei*	C	Anitápolis	SC/BR	L19	−27.902458	−49.129065
CFBH_20284	*Rhinella abei*	c1	Anitápolis	SC/BR	L19	−27.902458	−49.129065
CFBH_21056	*Rhinella crucifer*	N	Urucuca	BA/BR	L20	−14.586809	−39.291382
CFBH_21058	*Rhinella crucifer*	N	Urucuca	BA/BR	L20	−14.586809	−39.291382
CFBH_21113	*Rhinella crucifer*	N	Urucuca	BA/BR	L20	−14.586809	−39.291382
CFBH_21230	*Rhinella henseli*	S	Florianópolis	SC/BR	L21	−27.597024	−48.549583
CFBH_21317	*Rhinella abei*	c1	Guaratuba	SC/BR	L22	−25.883413	−48.576213
CFBH_22659	*Rhinella abei*	c1	Governador Celso Ramos	SC/BR	L23	−27.315793	−48.558841
CFBH_22816	Putative hybrid	H	Belo Horizonte	MG/BR	L24	−19.815731	−43.954223
CFBH_22897	*Rhinella abei*	c1	Morretes	PR/BR	L25	−25.476311	−48.835779
CFBH_23165	*Rhinella abei*	c1	Morretes	PR/BR	L25	−25.476311	−48.835779
CFBH_23166	*Rhinella abei*	c1	Morretes	PR/BR	L25	−25.476311	−48.835779
CFBH_23210	*Rhinella crucifer*	H	Vitória	ES/BR	L26	−20.322186	−40.338089
CFBH_23211	*Rhinella crucifer*	H	Conceicão da Barra	ES/BR	L27	−18.592569	−39.734653
CFBH_23368	*Rhinella crucifer*	N	Urucuca	BA/BR	L20	−14.586809	−39.291382
CFBH_23404	*Rhinella crucifer*	N	João Pessoa	PB/BR	L28	−7.115320	−34.861051
CFBH_23728	*Rhinella abei*	c1	Siderópolis	SC/BR	L29	−28.598892	−49.425409
CFBH_23729	*Rhinella abei*	c1	Siderópolis	SC/BR	L29	−28.598892	−49.425409
CFBH_23919	*Rhinella ornata*	C	Santos	SP/BR	L30	−23.961836	−46.332247
CFBH_2427	*Rhinella crucifer*	H	Conceicão da Barra	ES/BR	L27	−18.592569	−39.734653

Appendix 1. *Continued*

Collection no.	Species	Unit	Municipality	State/Country	Locality	Latitude	Longitude
CFBH_24271	*Rhinella ornata*	C	Derrubadas	RS/BR	L31	−27.265601	−53.861366
CFBH_24628	*Rhinella crucifer*	N	Camacan	BA/BR	L32	−15.414307	−39.500992
CFBH_24629	*Rhinella crucifer*	N	Camacan	BA/BR	L32	−15.414307	−39.500992
CFBH_24630	*Rhinella crucifer*	N	Camacan	BA/BR	L32	−15.414307	−39.500992
CFBH_2583	*Rhinella crucifer*	N	Ilhéus	BA/BR	L33	−14.729	−39.079
CFBH_27907	*Rhinella crucifer*	N	Palmeiras	BA/BR	L34	−12.529909	−41.575086
CFBH_27996	*Rhinella crucifer*	N	Santa Bárbara	BA/BR	L35	−11.957935	−38.967849
CFBH_28097	*Rhinella crucifer*	H	Santa Maria Madalena	RJ/BR	L36	−21.970085	−41.999240
CFBH_28098	*Rhinella crucifer*	H	Santa Maria Madalena	RJ/BR	L36	−21.970085	−41.999240
CFBH_28099	*Rhinella crucifer*	H	Santa Maria Madalena	RJ/BR	L36	−21.970085	−41.999240
CFBH_28100	*Rhinella crucifer*	H	Santa Maria Madalena	RJ/BR	L36	−21.970085	−41.999240
CFBH_28170	*Rhinella casconi*	G	Guaramiranga	CE/BR	L37	−4.271387	−38.946244
CFBH_28171	*Rhinella casconi*	G	Guaramiranga	CE/BR	L37	−4.271387	−38.946244
CFBH_28172	*Rhinella casconi*	G	Guaramiranga	CE/BR	L37	−4.271387	−38.946244
CFBH_28174	*Rhinella casconi*	G	Guaramiranga	CE/BR	L37	−4.271387	−38.946244
CFBH_28175	*Rhinella casconi*	G	Guaramiranga	CE/BR	L37	−4.271387	−38.946244
CFBH_2834	*Rhinella crucifer*	H	Aracruz	ES/BR	L38	−19.819578	−40.274341
CFBH_2837	*Rhinella abei*	c1	Morretes	PR/BR	L25	−25.476311	−48.835779
CFBH_2841	*Rhinella abei*	c1	Itapoá	SC/BR	L39	−26.117364	−48.616764
CFBH_2842	*Rhinella abei*	c1	Rio dos Cedros	SC/BR	L40	−26.738244	−49.272623
CFBH_2843	*Rhinella abei*	c1	Rio dos Cedros	SC/BR	L40	−26.738244	−49.272623
CFBH_2844	*Rhinella abei*	c1	Rio dos Cedros	SC/BR	L40	−26.738244	−49.272623
CFBH_2858	*Rhinella abei*	c1	Blumenau	SC/BR	L13	−26.918996	−49.066078
CFBH_2865	*Rhinella crucifer*	H	Aracruz	ES/BR	L38	−19.819578	−40.274341
CFBH_2866	*Rhinella crucifer*	H	Aracruz	ES/BR	L38	−19.819578	−40.274341
CFBH_2867	*Rhinella crucifer*	H	Aracruz	ES/BR	L38	−19.819578	−40.274341
CFBH_2869	*Rhinella crucifer*	H	Itaguaí	RJ/BR	L41	−22.866539	−43.777224
CFBH_2870	*Rhinella crucifer*	H	Itaguaí	RJ/BR	L41	−22.866539	−43.777224
CFBH_2871	*Rhinella crucifer*	H	Itaguaí	RJ/BR	L41	−22.866539	−43.777224
CFBH_2874	*Rhinella crucifer*	H	Vila Velha	ES/BR	L42	−20.330467	−40.292161
CFBH_2875	*Rhinella crucifer*	H	Vila Velha	ES/BR	L42	−20.330467	−40.292161
CFBH_2876	*Rhinella crucifer*	H	Vila Velha	ES/BR	L42	−20.330467	−40.292161
CFBH_2877	*Rhinella crucifer*	H	Vila Velha	ES/BR	L42	−20.330467	−40.292161
CFBH_2898	*Rhinella crucifer*	N	Ilhéus	BA/BR	L33	−14.729	−39.079
CFBH_2901	*Rhinella crucifer*	N	Ilhéus	BA/BR	L33	−14.729	−39.079
CFBH_2903	*Rhinella crucifer*	N	Ilhéus	BA/BR	L33	−14.729	−39.079
CFBH_2904	*Rhinella crucifer*	N	Ilhéus	BA/BR	L33	−14.729	−39.079
CFBH_2907	*Rhinella ornata*	C	Ubatuba	SP/BR	L1	−23.3433861	−45.085710
CFBH_2908	*Rhinella ornata*	C	Ubatuba	SP/BR	L1	−23.3433861	−45.085710
CFBH_2909	*Rhinella ornata*	C	Ubatuba	SP/BR	L1	−23.3433861	−45.085710
CFBH_2916	*Rhinella abei*	c1	Guaratuba	SC/BR	L22	−25.883413	−48.576213
CFBH_2918	*Rhinella abei*	c1	Guaratuba	SC/BR	L22	−25.883413	−48.576213
CFBH_326	*Rhinella ornata*	C	Ubatuba	SP/BR	L1	−23.3433861	−45.085710
CFBH_327	*Rhinella ornata*	C	Ubatuba	SP/BR	L1	−23.3433861	−45.085710
CFBH_328	*Rhinella ornata*	C	Ubatuba	SP/BR	L1	−23.3433861	−45.085710
CFBH_329	*Rhinella ornata*	C	Ubatuba	SP/BR	L1	−23.3433861	−45.085710
CFBH_3727	*Rhinella ornata*	C	Caraguatatuba	SP/BR	L43	−23.622528	−45.411901
CFBH_4177	*Rhinella crucifer*	H	Santa Teresa	ES/BR	L44	−19.931464	−40.595243
CFBH_5066	*Rhinella ornata*	H	Parati	RJ/BR	L4	−23.216708	−44.717938

Appendix 1. *Continued*

Collection no.	Species	Unit	Municipality	State/Country	Locality	Latitude	Longitude
CFBH_5081	*Rhinella ornata*	C	Rio Claro	SP/BR	L3	−22.413399	−47.569574
CFBH_5082	*Rhinella ornata*	C	Rio Claro	SP/BR	L3	−22.413399	−47.569574
CFBH_5083	*Rhinella ornata*	C	Rio Claro	SP/BR	L3	−22.413399	−47.569574
CFBH_5786	*Rhinella crucifer*	H	Parati	RJ/BR	L4	−23.216708	−44.717938
CFBH_6336	*Rhinella ornata*	C	Iporanga	SP/BR	L45	−23.439164	−47.424532
CFBH_6364	*Rhinella ornata*	C	Cananéia	SP/BR	L46	−25.024353	−47.932267
CFBH_6366	*Rhinella ornata*	C	Cananéia	SP/BR	L46	−25.024353	−47.932267
CFBH_6368	*Rhinella ornata*	C	Cananéia	SP/BR	L46	−25.024353	−47.932267
CFBH_6369	*Rhinella ornata*	C	Cananéia	SP/BR	L46	−25.024353	−47.932267
CFBH_6371	*Rhinella ornata*	C	Barra do Turvo	SP/BR	L47	−24.757996	−48.504925
CFBH_6372	*Rhinella ornata*	C	Barra do Turvo	SP/BR	L47	−24.757996	−48.504925
CFBH_6902	*Rhinella ornata*	C	Ribeirão Branco	SP/BR	L48	−24.219601	−48.767826
CFBH_6903	*Rhinella ornata*	C	Ribeirão Branco	SP/BR	L48	−24.219601	−48.767826
CFBH_7193	*Rhinella ornata*	C	Santo Antônio dos Pinhais	SP/BR	L49	−22.825353	−45.663319
CFBH_7194	*Rhinella ornata*	C	Santo Antônio dos Pinhais	SP/BR	L49	−22.825353	−45.663319
CFBH_725	*Rhinella ornata*	C	Jundiaí	SP/BR	L50	−23.186453	−46.884453
CFBH_726	*Rhinella ornata*	C	Jundiaí	SP/BR	L50	−23.186453	−46.884453
CFBH_727	*Rhinella ornata*	C	Jundiaí	SP/BR	L50	−23.186453	−46.884453
CFBH_7566	*Rhinella henseli*	S	São João do Triunfo	SC/BR	L51	−25.620462	−50.486946
CFBH_7665	*Rhinella ornata*	C	São Sebastião	SP/BR	L52	−23.761044	−45.412088
CFBH_7666	*Rhinella ornata*	C	São Sebastião	SP/BR	L52	−23.761044	−45.412088
CFBH_7753	*Rhinella ornata*	C	Ilha Bela	SP/BR	L8	−23.904000	−45.335000
CFBH_7754	*Rhinella ornata*	C	Ilha Bela	SP/BR	L8	−23.904000	−45.335000
CFBH_7755	*Rhinella ornata*	C	Ilha Bela	SP/BR	L8	−23.904000	−45.335000
CFBH_8353	*Rhinella ornata*	C	Rio Claro	SP/BR	L3	−22.413399	−47.569574
CFBH_8354	*Rhinella ornata*	C	Rio Claro	SP/BR	L3	−22.413399	−47.569574
CFBH_8355	*Rhinella ornata*	C	Rio Claro	SP/BR	L3	−22.413399	−47.569574
CFBH_8358	*Rhinella ornata*	C	Rio Claro	SP/BR	L3	−22.413399	−47.569574
CFBH_8359	*Rhinella ornata*	C	Rio Claro	SP/BR	L3	−22.413399	−47.569574
CFBH_8360	*Rhinella ornata*	C	Rio Claro	SP/BR	L3	−22.413399	−47.569574
CFBH_8458	*Rhinella abei*	c1	Itapema	SC/BR	L53	−27.090960	−48.611995
CFBH_8911	*Rhinella ornata*	C	São Luís do Paraitinga	SP/BR	L7	−23.228066	−45.322663
CFBH_958	*Rhinella crucifer*	H	Linhares	ES/BR	L11	−19.390915	−40.071503
CFBH_959	*Rhinella crucifer*	H	Linhares	ES/BR	L11	−19.390915	−40.071503
CFBH_9851	*Rhinella abei*	c1	Treviso	SC/BR	L54	−28.513920	−49.457338
CFBH_9937	*Putative hybrid*	C	Cristina	MG/BR	L6	−22.209178	−45.271985
CFBH_9965	*Rhinella henseli*	S	Anitápolis	SC/BR	L19	−27.902458	−49.129065
CFBH_9966	*Rhinella abei*	c1	Anitápolis	SC/BR	L19	−27.902458	−49.129065
IIBPH_1191	*Rhinella ornata*	C	Itapúa	IT/PAR	L55	−26.565580	−55.683650
IIBPH_1333	*Rhinella ornata*	C	Canindeyú	CA/PAR	L56	−24.137960	−55.668190
IIBPH_1342	*Rhinella ornata*	C	Itapúa	IT/PAR	L55	−26.565580	−55.683650
IIBPH_1563	*Rhinella ornata*	C	Itapúa	IT/PAR	L55	−24.137960	−55.668190
IIBPH_1564	*Rhinella ornata*	C	Itapúa	IT/PAR	L55	−24.137960	−55.668190
IIBPH_1565	*Rhinella ornata*	C	Itapúa	IT/PAR	L55	−24.137960	−55.668190
IIBPH_1566	*Rhinella ornata*	C	Itapúa	IT/PAR	L55	−26.565580	−55.683650
IIBPH_1567	*Rhinella ornata*	C	Itapúa	IT/PAR	L55	−24.137960	−55.668190
MZUSP_142100	*Rhinella inopina*	P	Januária	MG/BR	L57	−15.495640	−44.362592
MZUSP_142101	*Rhinella inopina*	P	Januária	MG/BR	L57	−15.495640	−44.362592
MZUSP_142105	*Rhinella inopina*	P	Januária	MG/BR	L57	−15.495640	−44.362592

Appendix 1. *Continued*

Collection no.	Species	Unit	Municipality	State/Country	Locality	Latitude	Longitude
MZUSP_142362	*Rhinella inopina*	P	Januária	MG/BR	L57	−15.495640	−44.362592
PUC_11666	Putative hybrid	H	Lima Duarte	MG/BR	L58	−21.848352	−43.807533
PUC_11667	Putative hybrid	H	Lima Duarte	MG/BR	L58	−21.848352	−43.807533
PUC_11671	Putative hybrid	H	Caeté	MG/BR	L59	−19.880666	−43.669804
PUC_11707	Putative hybrid	H	São Goncalo do Rio Preto	MG/BR	L60	−18.006592	−43.395201
PUC_11911	Putative hybrid	H	São Goncalo do Rio Abaixo	MG/BR	L61	−19.828069	−43.381984
PUC_11940	Putative hybrid	H	Nova Lima	MG/BR	L62	−19.987594	−43.846311
PUC_11941	Putative hybrid	H	Nova Lima	MG/BR	L62	−19.987594	−43.846311
PUC_11942	Putative hybrid	H	Nova Lima	MG/BR	L62	−19.987594	−43.846311
PUC_11943	Putative hybrid	H	Nova Lima	MG/BR	L62	−19.987594	−43.846311
PUC_11944	Putative hybrid	H	Nova Lima	MG/BR	L62	−19.987594	−43.846311
PUC_12035	Putative hybrid	H	Rio Piracicaba	MG/BR	L63	−19.926313	−43.169470
PUC_12565	Putative hybrid	H	Mar de Espanha	MG/BR	L64	−21.868582	−43.009314
PUC_1384	Putative hybrid	H	Joanésia	MG/BR	L65	−19.171585	−42.680580
PUC_1914	Putative hybrid	H	São Goncalo do Rio Abaixo	MG/BR	L61	−19.828069	−43.381984
PUC_1966	Putative hybrid	H	Serra do Caraca	MG/BR	L66	−20.133333	−43.500000
PUC_2841	Putative hybrid	H	Cariacica	ES/BR	L67	−20.265519	−40.420328
PUC_2842	Putative hybrid	H	Cariacica	ES/BR	L67	−20.265519	−40.420328
PUC_3150	Putative hybrid	H	Brumadinho	MG/BR	L68	−20.118182	−44.200950
PUC_3525	Putative hybrid	H	Belo Horizonte	MG/BR	L24	−19.815731	−43.954223
PUC_3526	Putative hybrid	H	Belo Horizonte	MG/BR	L24	−19.815731	−43.954223
PUC_3527	Putative hybrid	H	Belo Horizonte	MG/BR	L24	−19.815731	−43.954223
PUC_3528	Putative hybrid	H	Belo Horizonte	MG/BR	L24	−19.815731	−43.954223
PUC_3530	Putative hybrid	H	Belo Horizonte	MG/BR	L24	−19.815731	−43.954223
PUC_3534	Putative hybrid	H	Belo Horizonte	MG/BR	L24	−19.815731	−43.954223
PUC_3538	Putative hybrid	H	Belo Horizonte	MG/BR	L24	−19.815731	−43.954223
PUC_4023	Putative hybrid	N	Santa Maria do Salto	MG/BR	L69	−16.234376	−40.145041
PUC_4024	Putative hybrid	N	Santa Maria do Salto	MG/BR	L69	−16.234376	−40.145041
PUC_4977	Putative hybrid	H	Conceicão do Mato Dentro	MG/BR	L70	−19.042033	−43.417678
PUC_5143	Putative hybrid	H	Belo Horizonte	MG/BR	L24	−19.815731	−43.954223
PUC_5144	Putative hybrid	H	Belo Horizonte	MG/BR	L24	−19.815731	−43.954223
PUC_5176	Putative hybrid	H	Belo Horizonte	MG/BR	L24	−19.815731	−43.954223
PUC_5572	Putative hybrid	H	Belo Horizonte	MG/BR	L24	−19.815731	−43.954223
PUC_5693	Putative hybrid	H	Varginha	MG/BR	L71	−21.546379	−45.430813
PUC_5694	Putative hybrid	H	Varginha	MG/BR	L71	−21.546379	−45.430813
PUC_6003	Putative hybrid	H	Belo Horizonte	MG/BR	L24	−19.815731	−43.954223
PUC_6064	Putative hybrid	H	Juíz de Fora	MG/BR	L72	−21.764210	−43.349570
PUC_6178	Putative hybrid	N	Santa Maria do Salto	MG/BR	L69	−16.234376	−40.145041
PUC_6947	Putative hybrid	H	Conselheiro Lafaiete	MG/BR	L73	−20.659660	−43.785501
PUC_6959	Putative hybrid	H	Ouro Branco	MG/BR	L74	−20.517088	−43.700048
PUC_7534	Putative hybrid	N	Cristalia	MG/BR	L75	−16.754727	−42.908175
PUC_7535	Putative hybrid	N	Cristalia	MG/BR	L75	−16.754727	−42.908175
PUC_7536	Putative hybrid	N	Cristalia	MG/BR	L75	−16.754727	−42.908175
PUC_7537	Putative hybrid	N	Cristalia	MG/BR	L75	−16.754727	−42.908175
PUC_7538	Putative hybrid	N	Cristalia	MG/BR	L75	−16.754727	−42.908175

Appendix 1. *Continued*

Collection no.	Species	Unit	Municipality	State/Country	Locality	Latitude	Longitude
PUC_7539	Putative hybrid	N	Cristalia	MG/BR	L75	−16.754727	−42.908175
PUC_7540	Putative hybrid	N	Grão Mogol	MG/BR	L76	−16.557467	−42.893887
PUC_7551	Putative hybrid	H	Ouro Branco	MG/BR	L74	−20.517088	−43.700048
PUC_7552	Putative hybrid	H	Ouro Branco	MG/BR	L74	−20.517088	−43.700048
PUC_7553	Putative hybrid	H	Ouro Branco	MG/BR	L74	−20.517088	−43.700048
PUC_762	Putative hybrid	H	Caeté	MG/BR	L59	−19.880666	−43.669804
PUC_863	Putative hybrid	H	Caeté	MG/BR	L59	−19.880666	−43.669804
PUC_9445	Putative hybrid	H	Nova Lima	MG/BR	L62	−19.987594	−43.846311
PUC_962	Putative hybrid	H	Guanhães	MG/BR	L77	−18.771000	−42.931888
PUC_9705	Putative hybrid	N	São João do Paraíso	MG/BR	L78	−15.314933	−42.014371